doi: 10.4149/gpb_2017022

Ca^{2+}-dependent calcineurin/NFAT signaling in β-adrenergic-induced cardiac hypertrophy

Ali Khalilimeybodi[1], Alireza Daneshmehr[1] and Babak Sharif Kashani[2]

[1] *Department of Mechanical Engineering, College of Engineering, University of Tehran, Tehran, Iran*
[2] *Department of Cardiology, Massih-Daneshvari Hospital, Shahid Beheshti University of Medical Sciences, Tehran, Iran*

Abstract. Ca^{2+} is an important mediator in the β-adrenergic-induced cardiac hypertrophy. The β-adrenergic stimulation alters the Ca^{2+} transient characteristics including its oscillation frequency, diastolic and systolic levels which lead to the CaN activation and subsequent NFAT-dependent hypertrophic genes transcription. Moreover, β-adrenergic-induced alterations in PKA and GSK3β kinase activities in both the cytosol and the nucleus regulate NFAT nuclear translocation and contribute in its hypertrophic response. Due to the complex nature of CaN/NFAT signaling in cardiac cells, we use a computational approach to investigate the β-adrenergic-induced CaN/NFAT activation in the cardiac myocytes. The presented model predicts well the main physiological characteristics of CaN/NFAT signaling in accordance with the experimental observations. The presented model establishes the previous experimental and mathematical results on the principal role of Ca^{2+} oscillation frequency in the CaN/NFAT signaling and shows that increase in Ca^{2+} oscillation frequency enhances CaN activity and its sensitivity to low ISO concentrations. The model illustrates that in addition to the known ISO effect on Ca^{2+} transient amplitude, ISO-induced alterations in Ca^{2+} oscillation frequency, PKA and GSK3β kinase activities also greatly affect the β-adrenergic-induced NFAT activity. We also found that PKA has both pro-hypertrophic and anti-hypertrophic effects on NFAT activation and is the main kinase in ISO-induced NFAT activation.

Key words: β-adrenergic signaling — Hypertrophy — CaN/NFAT signaling — Ca^{2+} oscillation frequency — Protein kinase A

Abbreviations: Akt, protein kinase B (PKB); β-AR, β-adrenergic receptor; CaM, calmodulin; CaMKs, Ca^{2+}/calmodulin-dependent protein kinases; cAMP, cyclic adenosine monophosphate; CaN, calcineurin, GSK3β, glycogen synthase kinase 3 beta; ISO, isoproterenol; LTCCs, l-type Ca^{2+} channels; MCIP1, modulatory calcineurin-interacting protein 1; NFAT, nuclear factor of activated T cells; PKA, protein kinase A; PLB, phospholamban; RyRs, ryanodine receptors; SR, sarcoplasmic reticulum.

Introduction

The β-adrenergic signaling is one of the main players in the neurohumoral control of the heart which mediates various physiological and pathological responses (Saucerman and McCulloch 2006). In contrast to acute β-adrenergic stimulation which enhances cardiac functions, sustained β-adrenergic stimulation leads to the hypertrophy and

Electronic supplementary material. The online version of this article (doi: 10.4149/gpb_2017022) contains supplementary material, which is available to authorized users.

Correspondence to: Alireza Daneshmehr, Department of Mechanical Engineering, College of Engineering, University of Tehran, North Kargar St, Tehran, Iran
E-mail: Daneshmehr@ut.ac.ir

heart failure (Engelhardt et al. 1999). Ca^{2+} as a central second messenger in cardiomyocytes mediates a major part of β-adrenergic effects on cardiac functions and plays a fundamental role in the cardiac excitation-contraction (E-C) coupling (Zhang and Brown 2004). It is well established that alterations in intracellular calcium concentration regulate cardiomyocyte growth (hypertrophy), apoptosis and transcriptional gene expression (Fearnley et al. 2011; Kang 2013). Although initial changes in the cardiac calcium cycling are advantageous, they could be detrimental in heart failure (Roderick et al. 2007). The chronic changes in calcium signaling leads to the activation of transcription factors including the ones which cause hypertrophic genes expression (Molkentin 2006), in a process known as excitation–transcription (E-T) coupling (Zhang and Brown 2004).

Cardiac myocytes contain Ca^{2+}-dependent kinases and phosphatases which regulate E-T coupling (Dolmetsch 2003). Among them, Ca^{2+}/calmodulin-dependent protein kinases (CaMKs) and calcineurin (CaN) play the major role in transducing the hypertrophic signal (Bers 2008). CaMKII (δ isoform) is the predominant CaMK type in the heart (Colomer et al. 2003) which contributes to the regulation of calcium homeostasis and electrical activity in the heart (Onal et al. 2014). In the β-adrenergic signaling, due to the increased intracellular calcium level and heart rate, CaMKII activation is common (Erickson et al. 2011; Yang and Saucerman 2011), but its role in β-adrenergic-induced cardiac hypertrophy is controversial (Grimm and Brown 2010; Mattiazzi et al. 2015). On the other hand, CaN, a calcium- and calmodulin (CaM)-dependent serine/threonine phosphatase, is a well-established mediator for β-adrenergic-induced cardiac hypertrophy (Sanna et al. 2005; Shin et al. 2008). Upon activation by CaM, CaN dephosphorylates cytoplasmic nuclear factor of activated T cells (NFAT), a known hypertrophic transcription factor, and promotes its translocation to the nucleus and subsequent transcriptional activity. In contrast to CaN, several kinases such as glycogen synthase kinase 3 beta (GSK3β) and protein kinase A (PKA) phosphorylate NFAT in the cytosol and the nucleus and facilitate its nuclear export (Wilkins and Molkentin 2004).

The mechanism of CaN/NFAT activation in response to changes in intracellular calcium has been investigated thoroughly during last decades. But, due to the substantial complexity in calcium signaling in excitable cells such as cardiomyocytes, conventional experimental approaches have limitations in understanding the CaN/NFAT signaling in these cells (Goonasekera and Molkentin 2012). Nowadays, using systems biological approaches has been covered these shortcomings to an acceptable extent and provide an apparatus to investigate complex signaling networks such as CaN/NFAT signaling (Kang et al. 2016). In this regard, Fisher et al. (2006) simulated the NFAT activation in T lymphocytes (T cells) and showed that NFAT activity is not sensitive to the low frequencies of Ca^{2+} oscillations. They also demonstrated that Ca^{2+} oscillations could enhance the NFAT activity at low intracellular calcium level. In an ongoing research study (Shin et al. 2006, 2008, 2011), authors presented a mathematical model for NFAT cycling to study the dual regulatory role of MCIP1 in hypertrophic signaling. MCIP1 is a binding cofactor which its positive and negative regulatory effects on CaN activation have been reported (Shin et al. 2006). In a following study, Cui and Kaandrop (2008) expanded Shin's model (2006) to investigate calcium-CaN-MCIP1-NFAT signaling network in the cardiomyocytes for non-oscillatory calcium response. To capture the oscillatory nature of calcium handling in the heart, Cooling et al. (2009) presented a parsimonious model of CaN/NFAT signaling which replicates cardiac myocytes sensitivity to Ca^{2+} oscillations and CaN overexpression. Finally, in a recent study (Winslow et al. 2016), authors extended Saucerman-Bers model (Saucerman and Bers 2008) of Ca^{2+}-dependent signaling to capture the dynamics of NFAT activity and its transport to the nucleus. The authors showed that active NFAT in the nucleus is more sensitive to the frequency of Ca^{2+} transients rather than diastolic Ca^{2+}. Among the researchers that utilized computational approaches to investigate CaN/NFAT signaling, only Shin et al. (2011) take into account the CaN/NFAT activation by β-adrenergic signaling. Nevertheless, Shin and coauthors only constructed a minimal model of the main ERK and PI3K pathways of several hypertrophic signaling including β-adrenergic and did not consider Ca^{2+} oscillations and the role of PKA in the CaN/NFAT signaling (Shin et al. 2011).

The purpose of this study is to investigate the β-adrenergic-induced cardiac hypertrophy through the CaN/NFAT pathway. We consider the effects of β-adrenergic stimulation on the 1) frequency and amplitude of Ca^{2+} transient, 2) CaN activation by Ca^{2+}/CaM complex, 3) PKA and 4) GSK3β kinase activities in the cytosol and the nucleus, and 5) NFAT phosphorylation and translocation to the nucleus. We validate our results with available experimental data and results of systems studies that investigated CaN/NFAT signaling. We illustrate that ISO-induced increase in Ca^{2+} frequency comprises a considerable part of NFAT activation and increases the sensitivity of CaN activity to low ISO concentrations. Also, we show that PKA plays a greater role than GSK3β in regulating NFAT activity after β-adrenergic stimulation through activation and inhibition of NFAT *via* different mechanisms.

Materials and Method

The model of CaN/NFAT pathway in β-adrenergic signaling is shown schematically in Figure 1. The model involves

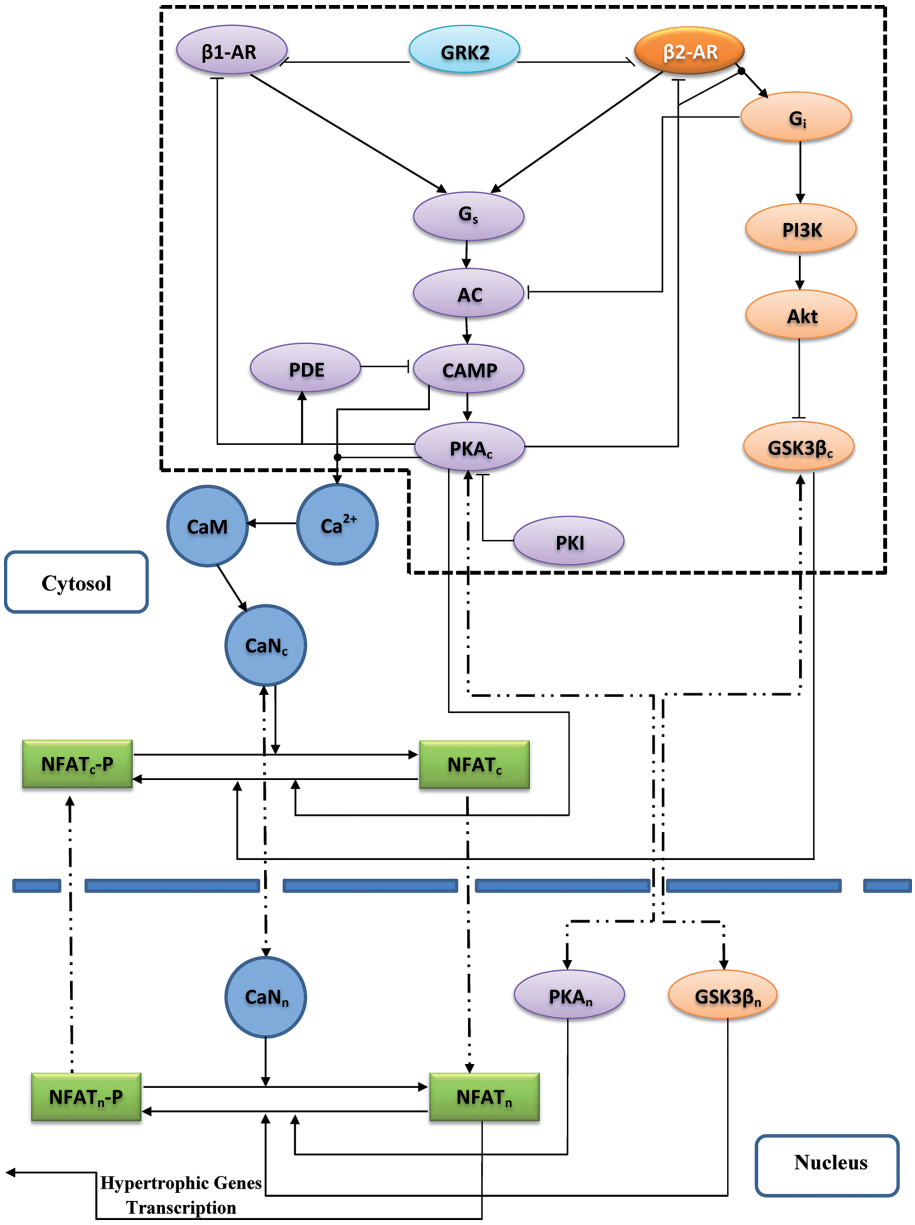

Figure 1. Schematic diagram of β-adrenergic signaling and CaN/NFAT pathway in the model. Cardiac myocyte is modeled in two compartments including the cytosol and the nucleus. Solid arrows represent kinetic reactions including mass action and Michaelis-Menten kinetics and dashed arrows illustrate nucleocytoplasmic shuttling of signaling components (β1-AR, β1-adrenergic receptor; β2-AR, β2-adrenergic receptor; GRK2, G protein-coupled receptor kinase 2; Gi, inhibitory G protein; PI3K, phosphoinositide 3-kinase; $GSK3\beta_c$, cytosolic GSK3β; $GSK3\beta_n$, nuclear GSK3β; Gs, stimulatory G protein; AC, adenylyl cyclase; PKA_c, cytosolic PKA; PKA_n, nuclear PKA; PDE, phosphodiesterase; PKI, protein kinase inhibitor; Ca^{2+}, cytosolic free calcium; CaN_c, cytosolic CaN; CaN_n, nuclear CaN; $NFAT_c$, cytosolic dephosphorylated NFAT; $NFAT_n$, nuclear dephosphorylated NFAT; $NFAT_c$-p, cytosolic phosphorylated NFAT; $NFAT_n$-p, nuclear phosphorylated NFAT). The area with dashed line perimeter shows the upstream β-adrenergic pathways that were developed in our previous study (Khalilimeybodi et al. 2017).

signaling components in two compartments: the cytosol and the nucleus. The model considers the ratio of nucleus to cytosol volume (~2% in mouse atrial and rat ventricular cells (Bers 2001)) in nucleocytoplasmic shuttling of signaling components.

In our previous study (Khalilimeybodi et al. 2017), we developed a computational model to investigate the effects of β-ARs stimulation through classical (Gs/Ac/cAMP/PKA) and non-classical (Gi/PI3K/Akt/GSK3β and Gi/Src/Ras/Raf/MEK/ERK) pathways on non Ca^{2+}-dependent hypertrophic transcription factors and validated our model with wide range of cardiac myocytes experimental data. In the current study, we used a part of our previous model to determine the ISO-induced variations of four mediators including cAMP, cytosolic PKA (PKA_c), double phosphorylated Akt (Akt-pp) which is the fully activated form of Akt and cytosolic GSK3β ($GSK3\beta_c$), see Fig. S1 in Supplementary Materials, to develop the model of Ca^{2+}-CaN/NFAT pathway in β-adrenergic signaling. The detailed description of our model for ISO-induced CaN/NFAT signaling (Fig. 1) and its equations and parameters are explained in Supplementary Materials.

The model of Ca^{2+}-dependent CaN/NFAT signaling comprises 15 state variables (Table S1) and 43 parameters (Table S2). Among the model parameters, 20 of them were

obtained directly from the literature and 23 of them were calibrated by fitting the simulated results to the experimental data through minimizing the objective function value which is sum of the squared residuals between experimental measurements and the model results. After developing the model equations, we use ode15s solver of MATLAB software to solve the system of ordinary differential equations. We obtain the initial conditions for state variables by running the model to steady-state without ISO stimulation, see Table S1 (Supplementary Materials).

Results and Discussion

β-adrenergic signaling effects on Ca^{2+} dynamics

In cardiac myocytes, Ca^{2+} response to different stimuli regulates many of cellular events such as growth, differentiation and excitation-contraction coupling. This response could be in different formats. Under specific circumstances, both level and frequency of the intracellular calcium are regulated by multiple stimuli including β-adrenergic receptor agonists. The β-AR-induced elevation in cytosolic Ca^{2+} level and frequency enhance cardiac contractility and hypertrophic signaling. However, differentiation between contractile Ca^{2+} oscillations and signaling Ca^{2+} is complicated and still not fully understood. In this regard, several hypotheses which consider regulation of signaling Ca^{2+} through increased Ca^{2+} amplitude, systolic level, diastolic level, and/or frequency are suggested (Goonasekera and Molkentin 2012). Investigating these hypotheses and various aspects of the complex β-AR-induced calcium signaling in cardiac myocytes requires utilization of a calcium transient model with relevant features. To do so, a simple modified model of calcium transient in the heart is presented. This model simulates calcium oscillations with different frequencies and reproduces the main characteristics of calcium transient in the cardiac myocytes as shown in Figure 2.

Ca^{2+} oscillation frequency plays a key role in transducing Ca^{2+} signals to hypertrophic effectors specially in CaN/NFAT signaling (Xia et al. 2000). So, calcium model should be able to predict the frequency-dependent response of cardiomyocytes Ca^{2+} transient, see Fig. 2A. In this regard, the presented model captures the variations of Ca^{2+} transient characteristics such as peak time, half-width, decay time constant, diastolic and systolic levels in response to the Ca^{2+} oscillation frequency. In general, there are considerable variations among experimental results from cardiomyocytes Ca^{2+} transient and the range of Ca^{2+} oscillations is wide (0.1–1 μM) (Bers 2001). Thus, we chose experimental data of frequency-dependent Ca^{2+} diastolic and systolic levels of mice cardiomyocytes (Pall et al. 2003) to estimate the modified model parameters. Then, we validated our model with comparing the simulated frequency-dependent aspects of cardiac Ca^{2+} transient with the experimental data. As seen from Fig. 2, the simulated responses are in line with the calcium experimental responses from mouse cardiac myocytes and calcium model is able to reproduce the relevant physiological phenomena.

On the one hand, due to the effects of pacing frequency on SR Ca^{2+} loading and Ca^{2+} release flux through RyRs (Bers 2001), increase in the Ca^{2+} oscillation frequency leads to the approximately linear elevation in both Ca^{2+} diastolic and systolic levels, but the effect of increased frequency on the amplitude of calcium transient (systolic minus diastolic levels) is less significant which is in accordance with Antoons et al. (2002) and Tavi et al. (2004) studies, see Fig. 2B. On the other hand, increased Ca^{2+} frequency results in the reduction of temporal characteristics of Ca^{2+} transient such as peak time (Fig. 2C), half-width (Fig. 2D) and decay time constant (Fig. 2E) which is a plausible adaptive response to increased frequency.

As shown in Fig. 2C, the increase in pacing frequency from 1 Hz to 8 Hz reduces Ca^{2+} transient peak time 21% and 19% in simulated and experimental results, respectively. For half-width, this reduction is 55% and 63%. For results on decay time constant, the simulated rate of reduction is more than experimental rate for frequencies below 3 Hz but for high frequencies, it closes to the experimental rate which is also seen in the Bondarenko (2014) study on cardiac Ca^{2+} transient. The frequency-dependent reduction of Ca^{2+} transient temporal characteristics is important in faster relaxation at higher heartbeats known as frequency-dependent acceleration of relaxation (FDAR) and allows the heart to refill faster than normal (Bers 2001).

Ca^{2+} transient in cardiac myocytes is not regulated only by variations in pacing frequency. The β-adrenergic receptors stimulation also contributes in regulating Ca^{2+} transient by modifying its amplitude and decay time. It is established that β-ARs stimulation by ISO enhances the amplitude and speeds up Ca^{2+} transient decline (Benkusky et al. 2007). The impacts of β-adrenergic signaling on Ca^{2+} transient are mediated mainly through cAMP and PKA which affects Ca^{2+} handling proteins such as LTCCs, PLB and RyRs. These modulations result in the more Ca^{2+} entering during excitation *via* LTCC phosphorylation and larger cytosolic Ca^{2+} uptake into SR during relaxation *via* PLB phosphorylation which is expected to increase SR Ca^{2+} load. The SR Ca^{2+} release could be enhanced by elevated Ca^{2+} current and SR Ca^{2+} load. All of these events results in the large increase in Ca^{2+} transient amplitude and rate of decline (Bers 2001).

Our model simulates the β-adrenergic signaling effects on Ca^{2+} transient in accordance with experimental results. As seen in Fig. 3A, the β-ARs stimulation by ISO (1 μM) leads to an increase in the Ca^{2+} systolic level. Also, it has been found

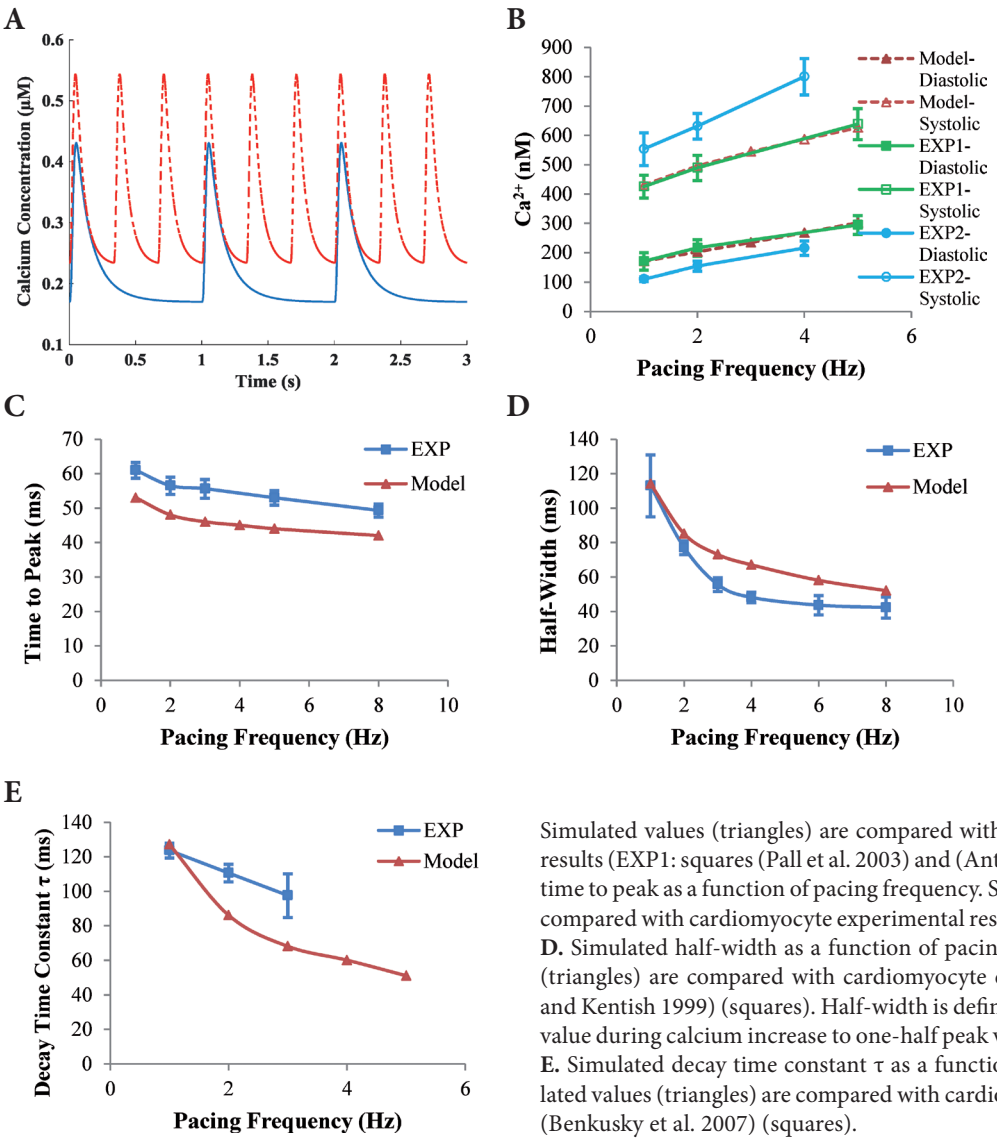

Figure 2. Simulated and experimental response of Ca^{2+} transient characteristics to pacing frequency in the cardiac myocytes. **A.** Simulated Ca^{2+} transients for 1 Hz (solid line) and 3 Hz (dashed line) stimulation. **B.** Diastolic and systolic calcium levels as a function of pacing frequency. Simulated values (triangles) are compared with cardiomyocyte experimental results (EXP1: squares (Pall et al. 2003) and (Antoons et al. 2002). **C.** Simulated time to peak as a function of pacing frequency. Simulated values (triangles) are compared with cardiomyocyte experimental results (Pall et al. 2003) (squares). **D.** Simulated half-width as a function of pacing frequency. Simulated values (triangles) are compared with cardiomyocyte experimental results (Layland and Kentish 1999) (squares). Half-width is defined as time from one-half peak value during calcium increase to one-half peak value during calcium decrease. **E.** Simulated decay time constant τ as a function of pacing frequency. Simulated values (triangles) are compared with cardiomyocyte experimental results (Benkusky et al. 2007) (squares).

that β-ARs stimulation does not change the Ca^{2+} diastolic level considerably (Despa et al. 2008; Knollmann et al. 2003; Song et al. 2012), that is in agreement with our simulations. After β-ARs stimulation, Ca^{2+} transient amplitude rapidly increases to its maximum in 150 s (Fig. 3B) and then slowly declines to its steady-state value (Fig. 3C). Despa (Despa et al. 2008) also record the similar transient response for ISO-induced Ca^{2+} amplitude. This transient response is due to the rapid initial activation of β-ARs and consequent elevation of intracellular cAMP level which raises Ca^{2+} systolic level and then β-ARs desensitization leads to the soft decline of systolic level to its steady-state.

To verify our model results on ISO-induced alterations in Ca^{2+} transient, we compare the simulation and experimental results of Ca^{2+} transient amplitude, and decay time constant after ISO stimulation. Fig. 3D compares the simulated and experimental results of the steady-state increase in Ca^{2+} transient amplitude after ISO stimulation. Our model predicts 3.96 and 3.23 amplification of Ca^{2+} amplitude in maximal and steady-state response of Ca^{2+} transient after β-ARs stimulation by 1 μM ISO, respectively.

In Fig. 3E, the simulated and experimental Ca^{2+} transient amplitude as a function of ISO concentration is illustrated. Also, after ISO stimulation (1 μM), the simulated Ca^{2+} transient decay time constants decrease from 127, 86 and 68 ms to 76, 59 and 50 ms at 1, 2 and 3 Hz pacing frequency, respectively. The ratios of simulated decay time constants without and with ISO stimulation at different pacing frequency are compared with experimental data in Fig. 3F. As shown in Figure 3, our model could reproduce the different

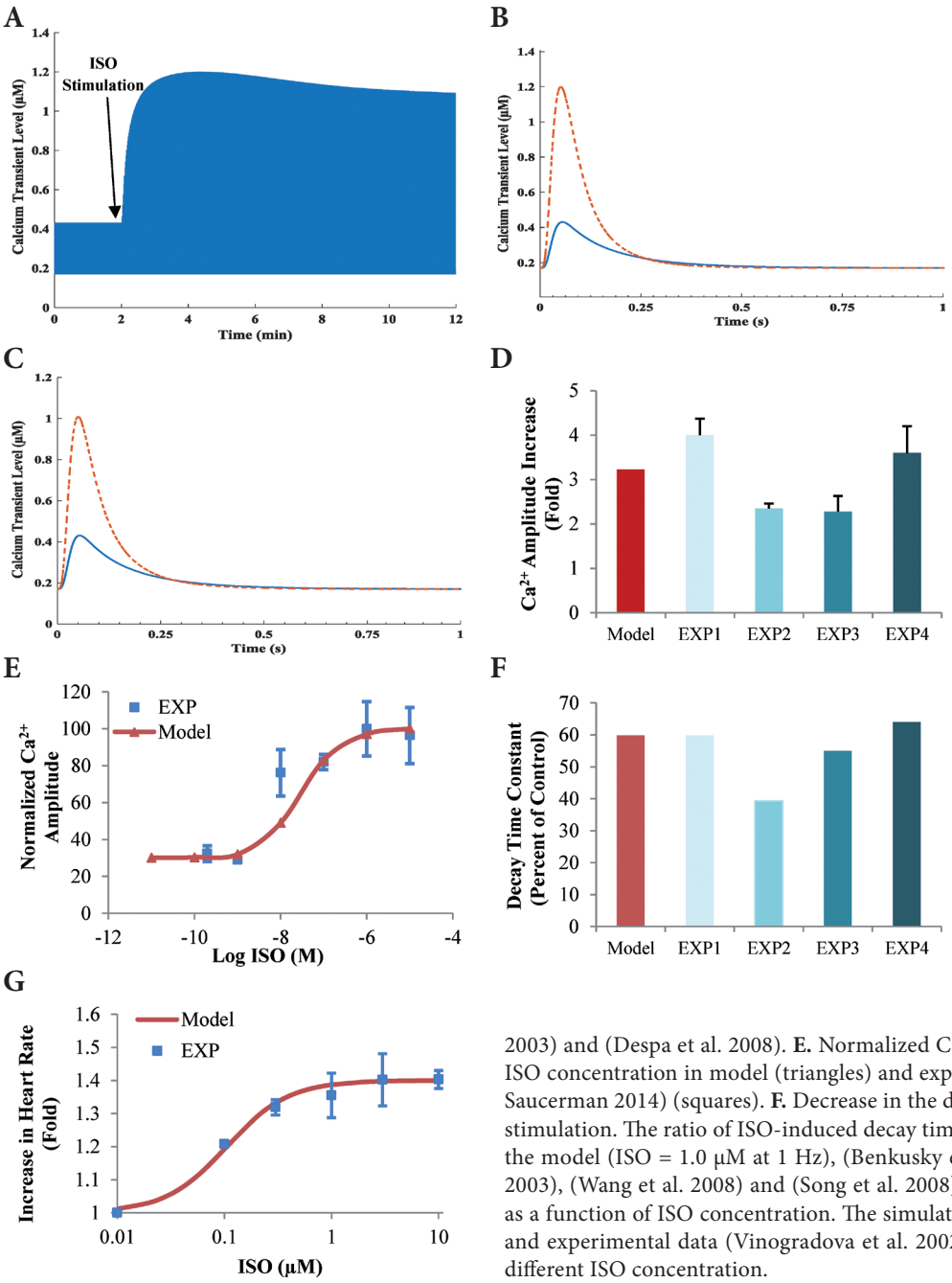

Figure 3. Simulated and experimental cardiac Ca^{2+} transient after β-ARs stimulation by ISO. **A.** Time course of Ca^{2+} transient before and after 1 μM ISO stimulation (at minute 2) at 1 Hz pacing frequency. **B.** Ca^{2+} transient with (dashed line) and without (solid line) ISO for one cycle time at maximal Ca^{2+} transient amplitude (150 s after stimulation). **C.** Ca^{2+} transient with (dashed line) and without (solid line) ISO for one cycle time after Ca^{2+} transient amplitude reaches to its ISO-induced steady-state value. **D.** Ca^{2+} transient amplitude amplification after ISO stimulation in the model (steady-state value: ISO = 1 μM at 1 Hz) and experimental results (Wang et al. 2008), (EXP2: ISO = 1 μM at 1 Hz, Liu et al. 2011), (Knollmann et al. 2003) and (Despa et al. 2008). **E.** Normalized Ca^{2+} amplitude as a function of ISO concentration in model (triangles) and experimental result (Amanfu and Saucerman 2014) (squares). **F.** Decrease in the decay time constant τ after ISO stimulation. The ratio of ISO-induced decay time constant to control value for the model (ISO = 1.0 μM at 1 Hz), (Benkusky et al. 2007), (Knollmann et al. 2003), (Wang et al. 2008) and (Song et al. 2008). **G.** Increase in the heartbeat as a function of ISO concentration. The simulated increase in heartbeat (line) and experimental data (Vinogradova et al. 2002) (squares) are illustrated for different ISO concentration.

physiological aspects of the β-ARs stimulation impacts on Ca^{2+} transient in consistent with the experimental data from cardiac myocytes.

In addition to alterations in Ca^{2+} transient amplitude and decay time, β-ARs stimulation results in the positive chronotropic (increased heartbeats) that calcium acts as an important player in its regulation. The experimental observations indicate that changes in Ca^{2+} SR release through RyR contributes in the β-adrenergic chronotropic effects in sinoatrial nodal pacemaker cells (SANCs) in the studied species (Vinogradova et al. 2002). Since the role of both Ca^{2+} transient level and frequency is established in CaN/NFAT signaling, we included the β-adrenergic effects on the heartbeat rate and Ca^{2+} frequency in our model. To do so, we obtained the equation for ISO-induced increase in the heartbeat (see Supplementary Materials, section 3) by fitting a sigmoid plot to the experimental results on ISO-induced changes in the heartbeat presented by Vinogradova et al.

(2002). The experimental data and our model predictions are illustrated in Fig. 3G. According to the Vinogradova et al. (2002) study, the heartbeat rapidly elevates to its steady-state value in 30 s after ISO stimulation which is very fast in comparison with frequency-dependent CaN activation time response. Thus, we do not consider this transient in our model.

β-AR-induced CaN activation

In contrast to the most hypertrophic mediators, it is established that CaN acts as both essential and sufficient mediator for pathological cardiac hypertrophy and could be activated by sustained increase in intracellular calcium level (Molkentin 2004). There are several hypotheses with experimental evidences about the main mechanism of Ca^{2+}-dependent CaN activation. One of them relates the CaN activation to the frequency of Ca^{2+} oscillations and considers CaN as an integrator of cardiac calcium signals (Colella et al. 2008; Colella and Pozzan 2008). The other relates it to the amplitude of the Ca^{2+} transient (Bers and Guo 2005). A hypothesis also explains that CaN responds to the sustained alterations in diastolic Ca^{2+} concentration rather than Ca^{2+} transient frequency or amplitude (Dolmetsch et al. 1997). But at present, the main mechanism is ambiguous due to the dependence between Ca^{2+} transient characteristic and difficulty in accurate measuring of these characteristics in beating cardiomyocytes. For example, elevating the Ca^{2+} transient frequency alters its diastolic level, systolic level, amplitude and the integral of Ca^{2+} transient (Goonasekera and Molkentin 2012). So, it is necessary to consider all of the Ca^{2+} transient alterations to fully analyze the Ca^{2+}-dependent CaN activation in β-adrenergic signaling.

As mentioned before, β-AR stimulation alters both Ca^{2+} transient frequency and amplitude and leads to the CaN activation (Zou et al. 2001). So, we analyzed the effects of Ca^{2+} intracellular level and its oscillation frequency on CaN activation in this section. As illustrated in Fig. 4A, activated CaN increases with the elevation of calcium intracellular concentration in both simulated and experimental results (Stemmer and Klee 1994). Also, with the increase in CaM total concentration, the plot shifts to the left and CaN will be activated at lower calcium concentration which could results in the cell hypertrophic response in the normal Ca^{2+} cycling. The experimental observation which indicates the cardiomyocytes growth and hypertrophy after overexpression of CaM supports this notion (Gruver et al. 1993).

In addition to increased calcium intracellular level, the elevation of Ca^{2+} transient frequency also leads to the CaN activation. As shown in Fig. 4B, the activated CaN accumulates to its steady-state value within 40 min and elevation in frequency results in the higher CaN activity. To analyze the mediators of this response, we compared the simulated frequency-induced CaN activation with constant

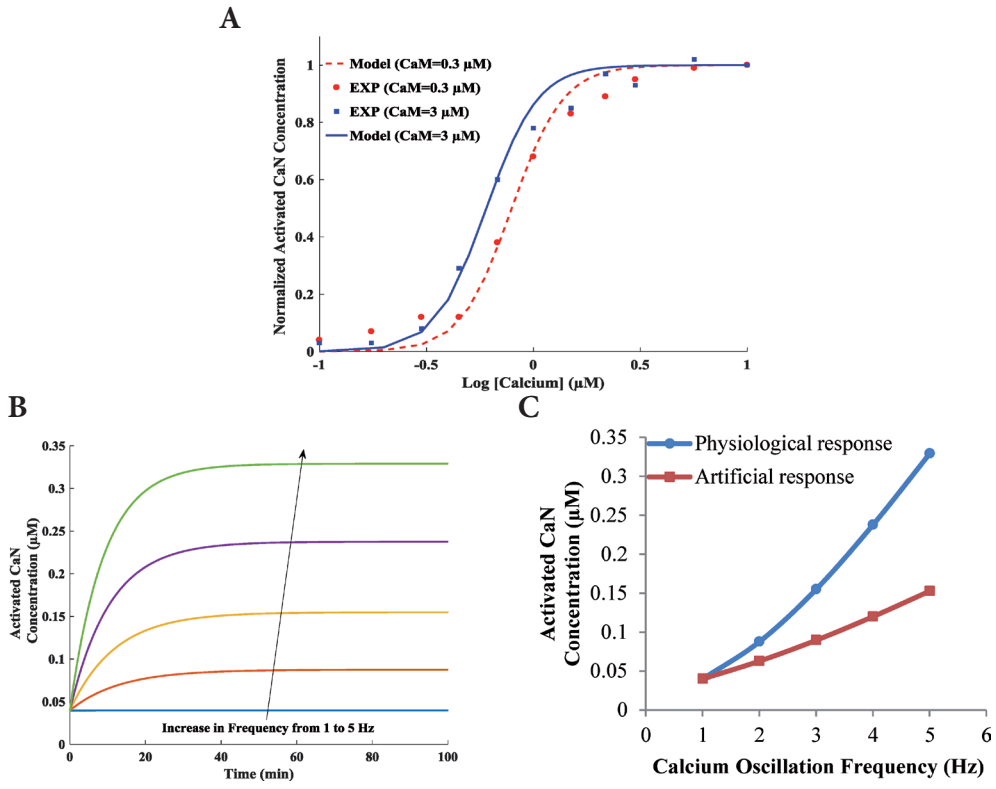

Figure 4. Ca^{2+}-dependent CaN activation. **A.** CaN activation as a function of intracellular Ca^{2+} concentration at different CaM concentration. The normalized concentration of activated CaN for CaM = 0.3 μM (dashed line) and 3 μM (solid line) in model are compared with experimental data for CaM = 0.3 μM (circles) and 3 μM (squares) of Stemmer and Klee (Stemmer and Klee 1994) study at different calcium concentration. **B.** Time course of simulated CaN activation at different pacing frequency (1–5 Hz). **C.** Comparison of CaN activation at physiological (circles) and artificial (without elevation in measured Ca^{2+} diastolic level: squares) conditions.

diastolic level, artificial response, with physiological CaN activation in Fig. 4C. Through comparing the steady-state CaN activations in Fig. 4C, we found that in addition to the frequency-induced elevation in Ca^{2+} measured diastolic level (responsible for 50–60% of CaN activation), integrating effect of Ca^{2+} transient frequency forms a considerable part of frequency-induced CaN activation which is also demonstrated in Tavi et al. (2004) and Saucerman and Bers (2008) studies. Actually, CaN activation after sustained increase in Ca^{2+} signal could be related to the elevation in the Ca^{2+} transient frequency which is responsible for increase in the integral of Ca^{2+} signal and subsequent elevation in effective Ca^{2+} diastolic level (Dolmetsch et al. 1997).

So far, we showed that in our model, CaN activation is dependent on both intracellular calcium level and oscillation frequency (Goonasekera and Molkentin 2012). In ISO-induced CaN activation, both of these factors act together. To investigate that, we simulated ISO-induced CaN activation in two states: (i) with and without ISO chronotropic response (Fig. 5A, B); (ii) at different pacing frequency (Fig. 5C, D).

As indicated in Fig. 5A, the CaN activity rises to its maximum value within 30 min and then decrease slowly to its steady-state value and this transient is more pronounced in high ISO concentration (greater than 10 nM). Figure 5B illustrates the CaN activation in response to ISO in two modes of stimulation: with and without ISO chronotropic response. In physiological mode, with chronotropic, the simulated values of CaN activation which were determined at 5 min and steady-state were compared with experimental results for different ISO concentration. According to the Fig. 5B, our model could predict the ISO-induced CaN activation in accordance with experimental results. Also, the comparison between CaN activities with and without ISO chronotropic response indicates that the chronotropic response to ISO forms a significant proportion of ISO-induced CaN activation in high ISO concentration due to the considerable increase in Ca^{2+} transient frequency, see Fig. 3G.

Since the Ca^{2+} oscillation frequency varies between different species, we analyzed the effect of Ca^{2+} transient frequency on ISO-induced CaN activation. According to the Fig. 5C, increase in the calcium frequency significantly shifts upwards the CaN activity dose-response curve to the more CaN activation. Also, as seen in Fig 5D, the elevated calcium frequency from 1 to 5 Hz increases the CaN sensitivity to low ISO concentration and decreases its EC_{50} from 42 nM to 22 nM. Since the effects of ISO on CaN activation mediates through the Ca^{2+} transient, it can be concluded that increasing Ca^{2+} frequency enhances the CaN activity at low intracellular Ca^{2+} level.

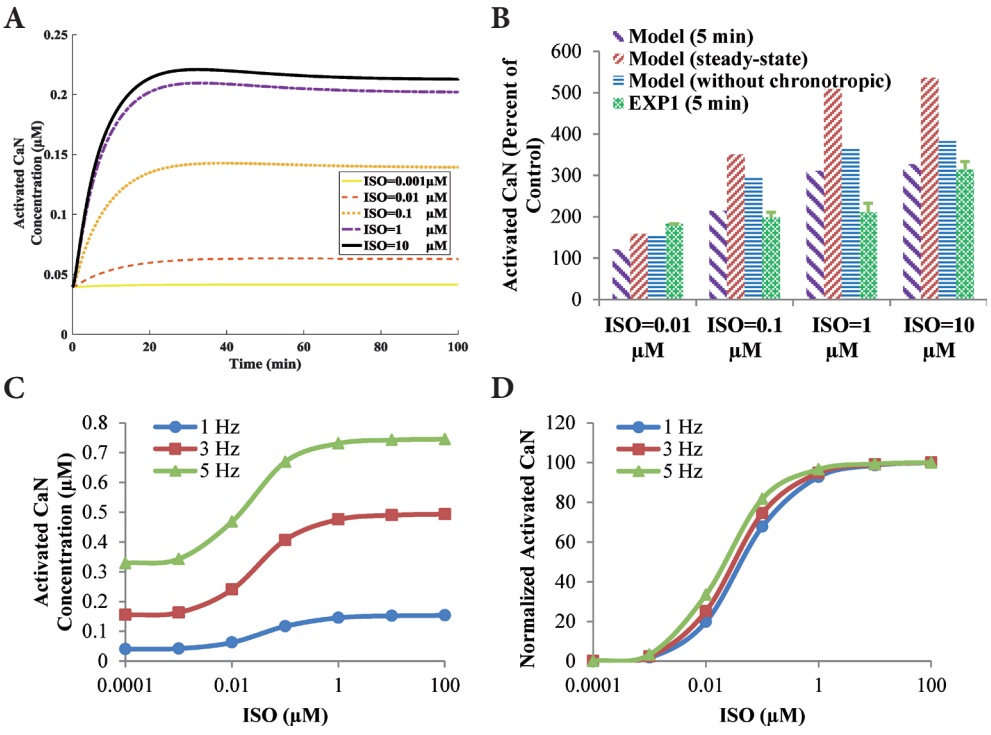

Figure 5. CaN activation after ISO stimulation. **A.** Time course of ISO-induced CaN activation with ISO chronotropic effect for different ISO concentrations with 1 Hz basal frequency for ISO = 0.001 to 10 μM. **B.** Increase in the simulated CaN activation in response to ISO stimulation with and without ISO chronotropic effect with 1 Hz basal frequency. The experimental data (Zou et al. 2001) (EXP1) are for CaN activation after 5 min stimulation at different ISO concentration with 1 Hz basal frequency. **C.** Activated CaN as a function of ISO concentration for different pacing frequencies. **D.** Normalized activated CaN (concentration of activated CaN) dose-response curves for different pacing frequencies. The simulated curves are at 1 Hz (circles), 3 Hz (squares) and 5 Hz (triangles) frequencies.

β-AR-induced NFAT activation

The activation of NFAT as a hypertrophic transcription factor is regulated by several factors in β-adrenergic signaling including: Ca^{2+} level and frequency through CaN activation, Akt/PI3K pathway through GSK3β inhibition and translocation, β-adrenergic classical pathway through Ca^{2+} transient modulation and PKA activation. Since GSK3β in both cytosol and nucleus play as the main kinase in regulating NFAT signaling, we estimated the GSK3β shuttling parameters to reproduce Shin et al. (2011) experimental data on GSK3β distribution in the H9C2 cells. In unstimulated cells as shown in Fig. 6A, endogenous GSK3β is mainly localized into the cytosol (nuclear/cytosol ratio: 0.21 ± 0.02). After pre-incubation with the PI3K-specific inhibitor LY294002 (LY29) or Crm1-specific inhibitor leptomycin B (LMB), GSK3β accumulates in the nucleus (nuclear/cytosol ratio for LY29: 0.82 ± 0.15 and LMB: 1.84 ± 0.11). LY29 inhibits Akt activation and its subsequent effects on GSK3β nuclear exit and LMB blocks GSK3β nuclear exit.

In the following, we calibrated our NFAT model to reproduce the experimental time course of total nuclear NFAT ($NFAT_n$ and $NFAT_{n\text{-}p}$) after electrical stimulation. Since the suitable NFAT signaling data for cardiac myocytes was unavailable, we used Shen et al. (2007) experimental data from skeletal myocytes which are excitable and similar to

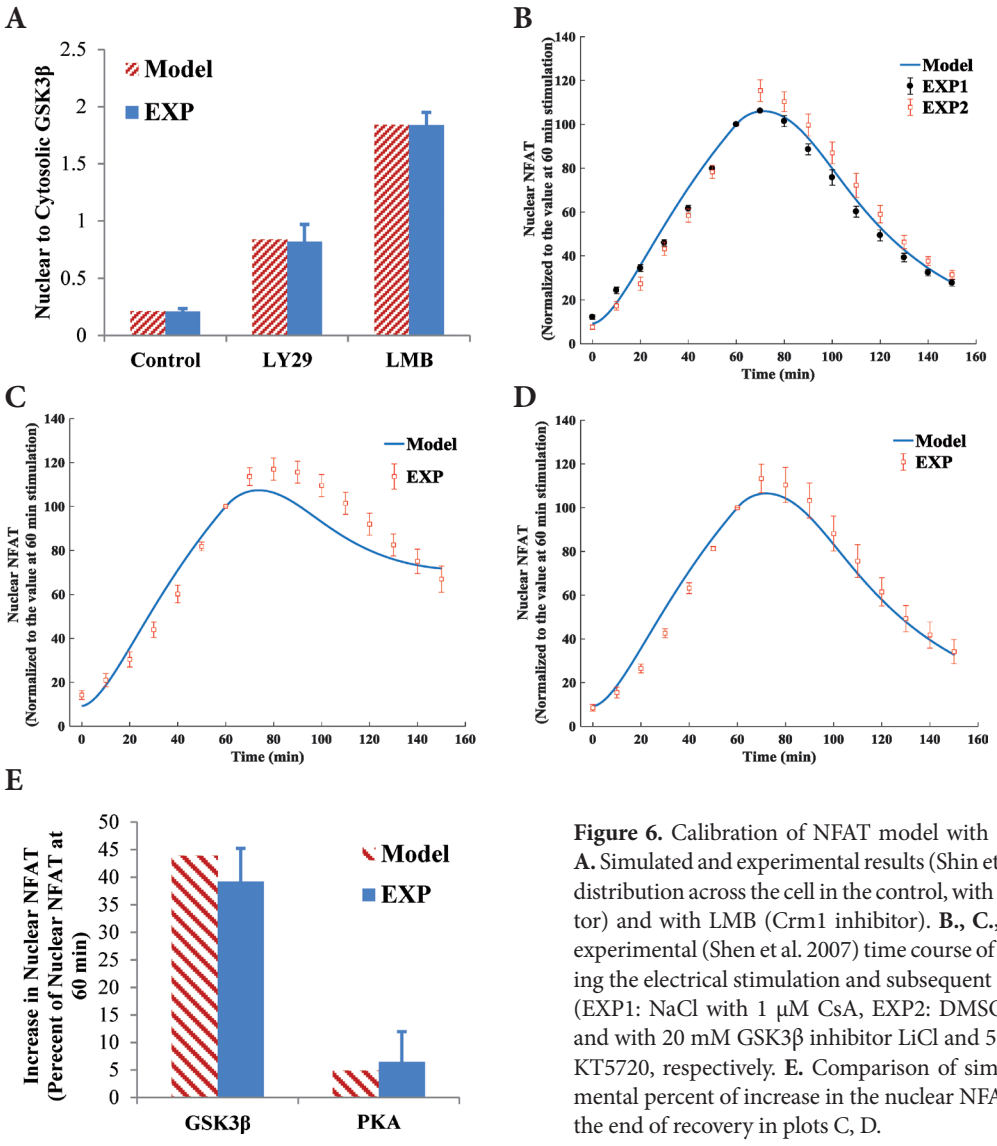

Figure 6. Calibration of NFAT model with experimental data. **A.** Simulated and experimental results (Shin et al. 2011) of GSK3β distribution across the cell in the control, with LY29 (PI3K inhibitor) and with LMB (Crm1 inhibitor). **B., C., D.** Simulated and experimental (Shen et al. 2007) time course of nuclear NFAT during the electrical stimulation and subsequent recovery in control (EXP1: NaCl with 1 μM CsA, EXP2: DMSO with 1 μM CsA) and with 20 mM GSK3β inhibitor LiCl and 5 μM PKA inhibitor KT5720, respectively. **E.** Comparison of simulated and experimental percent of increase in the nuclear NFAT concentration at the end of recovery in plots C, D.

cardiac myocytes from various aspects to estimate model parameters. As shown in Fig. 6B, 5 s train of 10 Hz stimuli with a period of 50 s for 60 min and subsequent 90 min recovery in the presence of the 1 μM CaN inhibitor cyclosporine A (CsA) results in a transient increase in nuclear NFAT during stimulation and its subsequent decline during the recovery. One of the characteristic of this transient response is the nuclear NFAT ongoing rise for 10 min after cessation of stimulation. As described in the Tomida et al. (2003) study, this behavior shows NFAT signaling ability to act as a memory for upstream Ca^{2+} signaling and independence of NFAT translocation to the nucleus from Ca^{2+} signaling. To obtain the main contributing parameter in this response, we accelerated the NFAT import to the nucleus or CaN deactivation by altering the related parameters. According to the results, accelerating the NFAT translocation to the nucleus slightly decreases the duration of nuclear NFAT increase after cessation of stimulation, but accelerating of CaN deactivation greatly diminishes this duration.

Also, we used Shen et al. (2007) experimental data on nuclear NFAT with the blockade of GSK3β and PKA activity to calibrate our model for kinase effects on NFAT signaling. Figures 6C and 6D illustrate the time course of nuclear NFAT in addition to the GSK3β and PKA inhibitor during recovery mode, respectively. As expected, inhibition of the GSK3β and PKA kinase activity results in the slower decline of nuclear NFAT than control and more nuclear accumulation of NFAT at the end of recovery time. As indicated in Fig. 6E, the role of GSK3β kinase activity in the NFAT regulation (39.2 ± 6% increase) is more effective than PKA (6.5 ± 5.5% increase) in their basal concentration.

To verify the model ability to predict NFAT activation after different stimulations by Ca^{2+} and analyze the effects of Ca^{2+} stimulation characteristics such as its duration and the interval of its repetition on NFAT activity, we compared the steady-state nuclear NFAT after two modes of stimulation by calcium with experimental results from Tomida et al. (2003) study on BHK cells, see Figs. 7A, B. We used the Ca^{2+} protocol in their study to simulate NFAT translocation to the nucleus. Since in the Tomida et al. (2003) study, nuclear NFAT comprises both phosphorylated and dephosphorylated NFAT, we used the total of these components as nuclear NFAT in simulated results in Figure 7. In the first mode, cells are stimulated by Ca^{2+} transient with 30 s duration at different intervals between 90 and 900 s.

According to the Fig. 7A, the simulated and experimental NFAT nuclear translocation decrease with the elevation of Ca^{2+} stimulation interval. This response confirms the experimental and mathematical results on the main role of Ca^{2+} oscillation frequency in NFAT activation (Dolmetsch et al. 1998; Fisher et al. 2006). Also, it shows that due to the difference in the kinetics of NFAT signaling such as

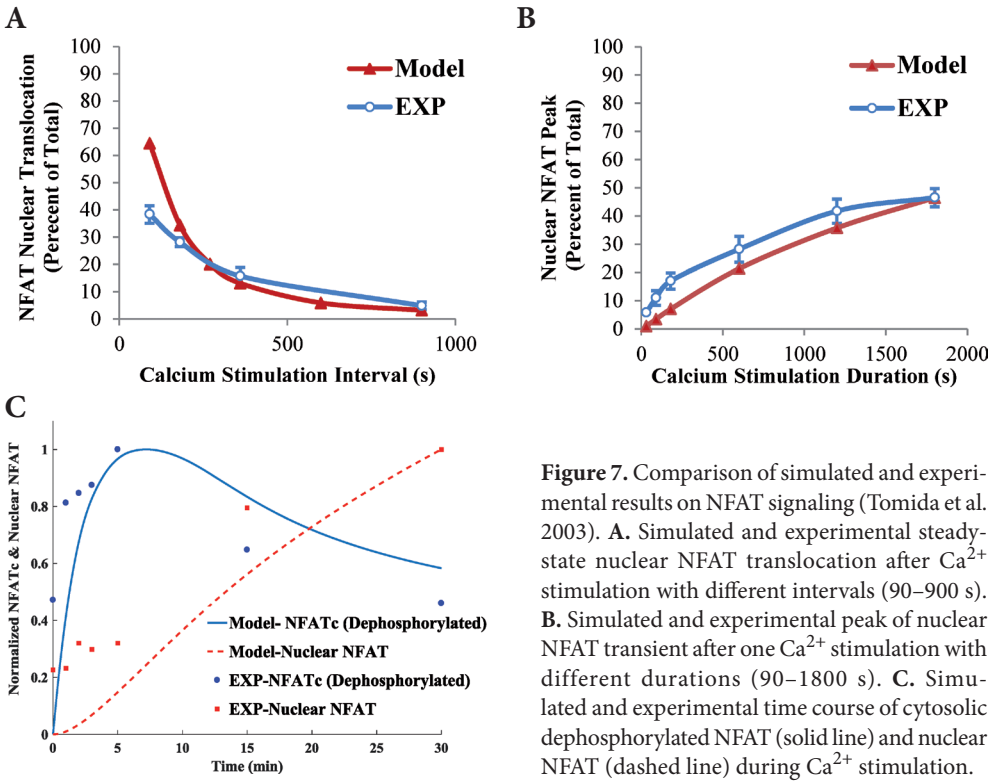

Figure 7. Comparison of simulated and experimental results on NFAT signaling (Tomida et al. 2003). **A.** Simulated and experimental steady-state nuclear NFAT translocation after Ca^{2+} stimulation with different intervals (90–900 s). **B.** Simulated and experimental peak of nuclear NFAT transient after one Ca^{2+} stimulation with different durations (90–1800 s). **C.** Simulated and experimental time course of cytosolic dephosphorylated NFAT (solid line) and nuclear NFAT (dashed line) during Ca^{2+} stimulation.

NFAT fast dephosphorylation, slow rephosphorylation and extremely slow nuclear translocation; NFAT will be significantly activated if the Ca^{2+} stimulation interval is shorter than dephosphorylated NFAT lifetime (Tomida et al. 2003).

In the second mode, cells were stimulated *via* a single Ca^{2+} transient with different duration from 90 to 1800 s. As seen from Fig. 7B, increase in the Ca^{2+} transient duration results in the increase in the peak concentration of nuclear NFAT. This response is expected due to the more CaN activation and consequent more NFAT dephosphorylation and translocation to the nucleus when there is more sustained calcium stimulation. Although our model was calibrated by Shen et al. (2007) results on the skeletal myocytes which is different with Tomida et al. (2003) study on BHK cells in various aspects, our model results are consistent with experimental data to an acceptable level.

Also, Tomida et al. (2003) showed that because of the mentioned different in NFAT signaling kinetics, dephosphorylated NFAT initially accumulates in the cytosol during Ca^{2+} stimulation and then its translocation to the nucleus results in its reduction. Figure 7C illustrates the simulated and experimental time course of cytosolic dephosphorylated NFAT ($NFAT_c$) and nuclear NFAT during Ca^{2+} stimulation for 30 min. Despite the differences between quantitative results, our model prediction of $NFAT_c$ and nuclear NFAT time course are qualitatively similar to Tomida et al. (2003) results. Cooling et al. (2009) suggested that this difference (returning $NFAT_c$ concentration to its initial value after 30 min even with ongoing Ca^{2+} stimulation) could be due to the neglecting the inhibitory effects of MCIP1 as a NFAT signaling regulator. But in the NFAT signaling model by Shin et al. (2006) which specifically studies the role of MCIP1 in NFAT signaling, the authors showed that MCIP1 affects cytosolic NFAT with a significant delay and despite its inhibitory effect, $NFAT_c$ does not come back to its initial value. Thus, MCIP1 could not produce an $NFAT_c$ time course same as experimental one in Fig. 7C and there must be factors other than MCIP1 for making this response. The other disagreement between our model result and experiment in Fig. 7C is the initial conditions issue. Although, first, we run the model without ISO stimulation to obtain nonzero values for our model initial conditions, the obtained values are not similar to the initial conditions in experiment. This disagreement has many reasons, but the main reasons are 1) not considering other cellular components and reactions which regulate the concentration of a specific component in the cell and 2) the specific experimental conditions for every experimental data.

So far, we showed that our model could predict NFAT activation in response to alterations in calcium transient characteristics such as calcium interval and duration in accordance with experimental results. In the following, the sensitivity of dephosphorylated nuclear NFAT ($NFAT_n$), the responsible component for gene transcription, to calcium

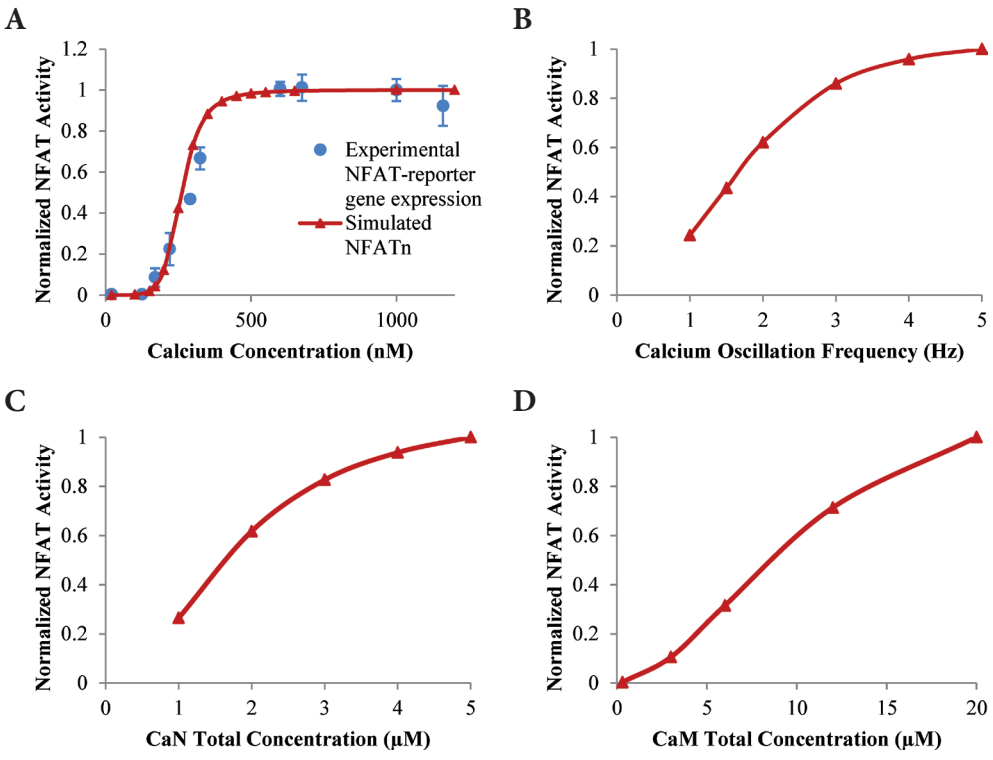

Figure 8. Sensitivity of NFAT activity to its mediators. **A.** Comparison of simulated steady-state NFATn and experimental NFAT- reporter gene expression (Dolmetsch et al. 1998) sensitivities to Ca^{2+} concentration for constant calcium stimulation. Data are normalized to the value at 1000 nM calcium concentration (Model: triangles, EXP: circles). **B.** Simulated NFATn steady-state concentration as a function of Ca^{2+} frequency. **C.** Simulated NFATn steady-state concentration as a function of CaN total concentration. **D.** Simulated NFATn steady-state concentration as a function of CaM total concentration.

concentration for constant Ca^{2+} stimulation is illustrated in Fig. 8A. Despite a little more sensitivity to calcium level in the simulated results than experimental data (Model: EC_{50} = 263 nM, EXP: EC_{50} = 295 nM), our model results are in good agreement with experimental NFAT-reporter gene expressions from Dolmetsch et al. (1998) study on Jurkat T cells. Also, the dependence of steady-state concentration of $NFAT_n$ to Ca^{2+} frequency is displayed in Fig. 8B. As expected, increase in the Ca^{2+} frequency (involving increase in Ca^{2+} diastolic level) results in the more NFAT nuclear localization and more hypertrophic gene transcription by $NFAT_n$ (Goonasekera and Molkentin 2012).

Several experimental studies demonstrated that overexpression of CaM or CaN without alteration in Ca^{2+} transient results in the NFAT translocation to the nucleus and its activation (O'Keefe et al. 1992; Gruver et al. 1993). To investigate this subject by our model, we simulate NFAT activity in the presence of different total concentration of CaM and CaN. As shown in Figs. 8C and D, CaN and CaM overexpression leads to the substantial increase in the NFAT activity. The 2-fold increase in the nominal total concentration of CaN and CaM in our model results in the 2.33-fold and 2.26-fold increase in the NFAT activity, respectively.

ISO stimulation affects NFAT signaling through different mediators including CaN, PKA and GSK3β. As mentioned earlier, in the CaN activation by ISO, both Ca^{2+} frequency and amplitude elevation contribute in CaN activation and consequently NFAT activation. As shown in Fig. 3G, maximum ISO stimulation results in the 1.4-fold increase in Ca^{2+} frequency. According to the Fig. 8B, in cells with 1, 2, and 3 Hz base frequency, maximum ISO stimulation results in the 1.626, 1.32 and 1.128-fold increase in the $NFAT_n$ concentration, respectively. To determine the contribution of ISO chronotropic response in ISO-induce NFAT activation, the dose-response of NFAT activity ($NFAT_n$ concentration) with and without ISO chronotropic response with 1 Hz Ca^{2+} base frequency is illustrated in Fig. 9A. According to this figure, in maximum ISO stimulation, ISO chronotropic effect amplifies NFAT activity ($NFAT_n$ concentration) 1.15-fold. Also, the ISO chronotropic effect on NFAT activity is distinguishable only for ISO concentrations higher than 10 nM and could be neglected in the low ISO stimulations.

In addition to the effect of ISO on Ca^{2+} frequency, the dose-response of NFAT activity with and without ISO effects on PI3K/GSK3β pathway (by blocking ISO-induced Akt activation) is illustrated in Fig. 9B to obtain the GSK3β contribution in ISO-induced NFAT nuclear translocation and activity. The PI3K/Akt activation by ISO decreases the GSK3β kinase activity in the cytosol and the nucleus by GSK3β phosphorylation and nuclear export, respectively. This reduction attenuates GSK3β inhibitory effect on NFAT signaling in both the cytosol and the nucleus which renders the increase in $NFAT_n$ concentration and transcriptional

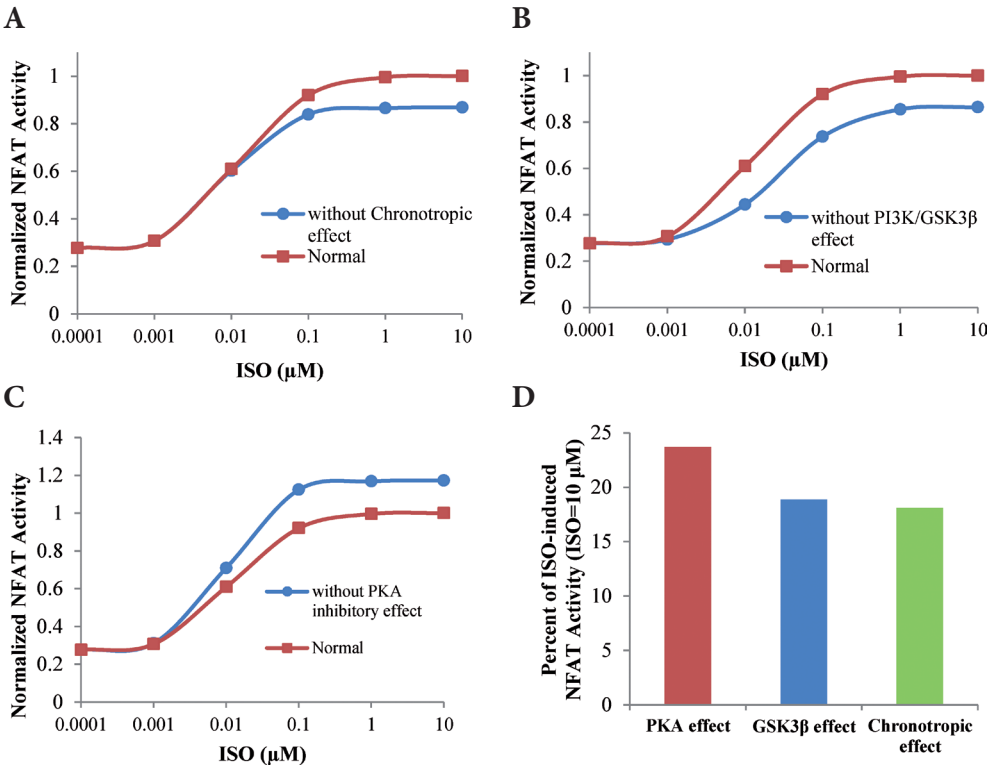

Figure 9. Comparison of simulated dose-response of steady-state NFAT activity in normal condition with artificial conditions. **A.** Blocking ISO effects on Ca^{2+} frequency (chronotropic effect). **B.** Blocking the effect of ISO stimulation on GSK3β kinase activity through PI3K/Akt pathway by blocking ISO-induced Akt activity. This results in more active GSK3β and its inhibitory effects on NFAT activity. **C.** Blocking the inhibitory effects of PKA on NFAT signaling after ISO stimulation. The effects of PKA on Ca^{2+} transient after ISO stimulation (its prohypertrophic effects) is not blocked in panel C. **D.** Contribution of PKA and GSK3β effects and increase in Ca^{2+} frequency on ISO-induced NFAT activity at maximum ISO stimulation (10 μM).

activity in normal state as shown in Fig. 9B. The effect of GSK3β on NFAT activity is nearly equal to the chronotropic effect of ISO in high ISO stimulations (greater than 1 μM). But, in contrast to ISO effect on Ca^{2+} frequency, its effect on GSK3β influences NFAT transcriptional activation even in the low concentrations of ISO.

Most of the studies on the NFAT signaling emphasize on the GSK3β influence on NFAT rephosphorylation rather than PKA. But, in the ISO-induced NFAT activation due to the substantial increase in the PKA kinase activity, it seems that PKA plays the major role. We simulated the ISO-induced NFAT activity as a function of ISO concentrations with and without PKA inhibitory effect on NFAT rephosphorylation in Fig. 9C and compared its effect on NFAT activity with GSK3β and ISO chronotropic effects in Fig. 9D. PKA has a greater influence on the ISO-induced NFAT activity than GSK3β (23.7% *vs.* 18.9%), but their difference is not significant. Also, the main effect of PKA activation on NFAT activity is through Ca^{2+} amplitude amplification and consequent CaN activation. Therefore, PKA has a far greater effect than GSK3β in ISO-induced NFAT activity. Moreover, our model predicts 3.63-fold increase in steady-state $NFAT_n$ concentration after maximum ISO stimulation in normal state which is in the experimental range of ISO-induced NFAT translocation to the nucleus (1.85-fold increase in rat cardiomyocytes (Dai et al. 2014) and 4.5-fold increase in mice cardiomyocytes (Li et al. 2014)).

To analyze the ISO-induced NFAT activation, we illustrated the time course of NFAT model components during 1 μM ISO stimulation with 1 Hz Ca^{2+} base frequency in Figure 10. On the one hand, after ISO stimulation, the cytosolic phosphorylated NFAT ($NFAT_{c\text{-}p}$) dephosphorylates into the cytosolic NFAT ($NFAT_c$) through increase in the CaN activation and decrease in the $GSK3\beta_c$ inhibitory effect and its concentration decreases slowly to its steady-state value. But, $NFAT_c$ concentration rapidly elevates to its maximum due to the fast kinetic of NFAT dephosphorylation and then slowly translocates to the nucleus, see Fig. 10A. On the other hand, NFATn slowly accumulates in the nucleus but phosphorylated nuclear NFAT ($NFAT_{n\text{-}p}$) initially decreases due to the fast CaN_n activation and $GSK3\beta_n$ nuclear exit and then slowly elevates to its steady-state value due to the increase in the PKA_n activation and $NFAT_n$ accumulation as shown in the Fig. 10B. In contrast to the slower activation of PKA in the nucleus than cytosol due to its slow diffusion through the nucleus (Fig. 10C), $GSK3\beta_n$ concentration declines faster than $GSK3\beta_c$ due to the Aktpp-induced promotion of GSK3β nuclear exit (Fig. 10D) (Shin et al. 2011).

Despite our model ability to predict correctly the main physiological responses of NFAT signaling and reproduce the available experimental data on different cells with oscillatory Ca^{2+}, the model has several limitations. Firstly, we could not determine our model abilities to predict NFAT signaling response in cardiomyocytes due to unavailability of suitable

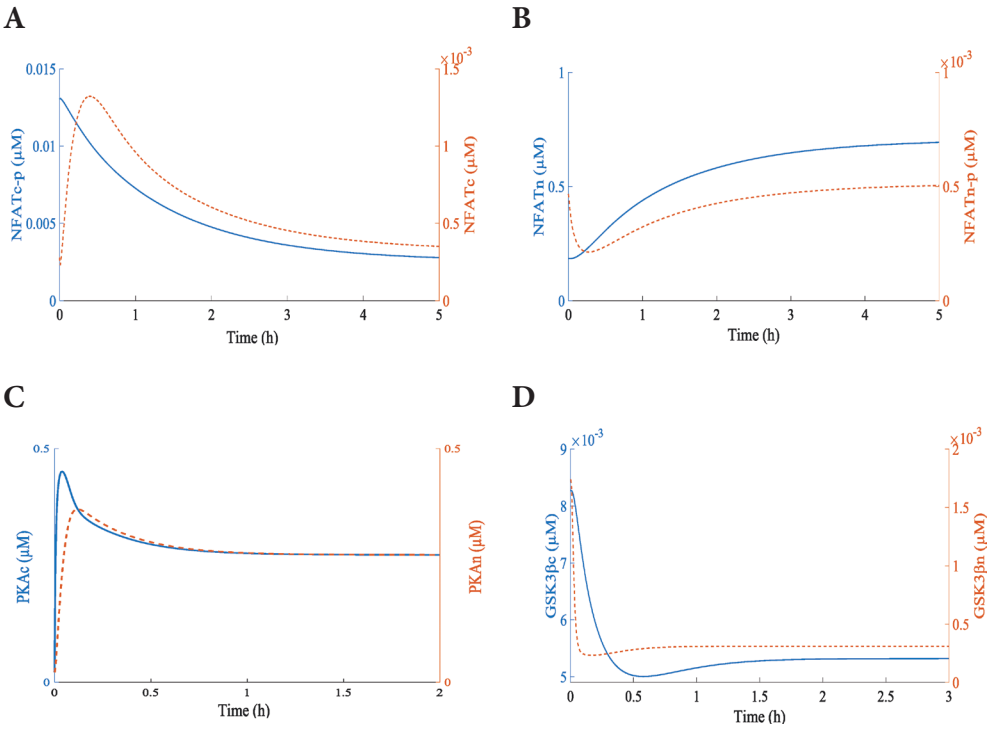

Figure 10. Time course of NFAT signaling components after ISO (1 μM) stimulation. **A.** Cytosolic phosphorylated (NFATc-p: solid line) and dephosphorylated NFAT (NFATc: dashed line) time course. **B.** Nuclear phosphorylated (NFATn-p: dashed line) and dephosphorylated NFAT (NFATn: solid line) time course. **C.** Cytosolic PKA (PKAc: solid line) and nuclear PKA (PKAn: dashed line) catalytic subunit time course. **D.** Cytosolic GSK3β (GSK3βc: solid line) and nuclear GSK3β (GSK3βn: dashed line) time course.

cardiomyocytes experimental data for NFAT signaling which consider Ca^{2+} frequency. Secondly, there are other regulators in ISO-induced NFAT activation such as MCIP1, ERK5 and Atrogin1 (Shin et al. 2008) that are not considered in our model due to their little or complex influences on ISO-induced NFAT activity and could affect the accuracy of our model to predict CaN/NFAT signaling responses. Thirdly, for the sake of simplicity, we do not consider the buffering ability of Ca^{2+}-binding components like troponin C (TnC) in our model that could influence the Ca^{2+}/CaM signaling and consequently CaN/NFAT signaling. Finally, several researchers indicated that excitation-transcription coupling in the heart is mainly mediated by Ca^{2+} transient in the specific compartments of cardiac myocytes rather than free cytosolic Ca^{2+} transient (Saucerman and Bers 2008). One of these compartments is dyadic cleft which its Ca^{2+} transient has an extremely high amplitude (Saucerman and Bers 2008). But, Saucerman and Bers showed that in beating myocytes, CaN is constitutively active in dyadic cleft compartment and could not be a mediator for hypertrophic signals. Another important compartment is the nucleus which, as mentioned earlier, is not a notable compartment in ISO-induced NFAT activity. So, this limitation is not a significant problem for our specific subject.

Conclusion

In the current study, we presented a computational model to investigate β-adrenergic-induced cardiac hypertrophy through Ca^{2+}-dependent CaN/NFAT signaling. The model is calibrated and verified against the experimental data to predict the CaN/NFAT response to Ca^{2+} transient characteristics including its oscillation frequency and amplitude. We examined the different hypotheses about transducing Ca^{2+} signaling in the background of Ca^{2+} oscillation and showed that Ca^{2+} frequency plays a significant role in the CaN/NFAT activation and CaN and NFAT act as an integrator and a memory for their upstream Ca^{2+} signaling, respectively. We determined the contribution of different mediators in ISO-induced NFAT activation such as GSK3β and PKA and the contribution of ISO chronotropic response in CaN and NFAT activation. By comparing the mediators' contribution, we also showed that in unstimulated cells, GSK3β is the main kinase in regulating NFAT signaling, but after ISO stimulation PKA plays this role.

Acknowledgement. We convey our thanks to Dr. M. Dehghani for his great help.

Conflict of interest. All of the authors declare that there is no conflict of interest regarding the publication of this article.

References

Amanfu RK, Saucerman JJ (2014): Modeling the effects of β1-adrenergic receptor blockers and polymorphisms on cardiac myocyte Ca2+ handling. Mol. Pharmacol. **86,** 222–230 https://doi.org/10.1124/mol.113.090951

Antoons G, Mubagwa K, Nevelsteen I, Sipido KR (2002): Mechanisms underlying the frequency dependence of contraction and [Ca2+]i transients in mouse ventricular myocytes. J. Physiol. **543,** 889–898 https://doi.org/10.1113/jphysiol.2002.025619

Benkusky NA, Weber CS, Scherman JA, Farrell EF, Hacker TA, John MC, Powers PA, Valdivia HH (2007): Intact β-adrenergic response and unmodified progression toward heart failure in mice with genetic ablation of a major protein kinase A phosphorylation site in the cardiac ryanodine receptor. Circ. Res. **101,** 819–829 https://doi.org/10.1161/CIRCRESAHA.107.153007

Bers D (2001): Excitation-Contraction Coupling and Cardiac Contractile Force. Vol. **237,** Springer Science & Business Media https://doi.org/10.1007/978-94-010-0658-3

Bers DM, Guo T (2005): Calcium signaling in cardiac ventricular myocytes. Ann. N.Y. Acad. Sci. **1047,** 86–98 https://doi.org/10.1196/annals.1341.008

Bers DM (2008): Calcium cycling and signaling in cardiac myocytes. Annu Rev. Physiol. **70,** 23–49 https://doi.org/10.1146/annurev.physiol.70.113006.100455

Bondarenko VE (2014): A compartmentalized mathematical model of the β1-adrenergic signaling system in mouse ventricular myocytes. PloS One **9,** e89113 https://doi.org/10.1371/journal.pone.0089113

Colella M, Grisan F, Robert V, Turner JD, Thomas AP, Pozzan T (2008): Ca2+ oscillation frequency decoding in cardiac cell hypertrophy: role of calcineurin/NFAT as Ca2+ signal integrators. Proc. Natl. Acad. Sci. USA **105,** 2859–2864 https://doi.org/10.1073/pnas.0712316105

Colella M, Pozzan T (2008): Cardiac cell hypertrophy in vitro. Ann. NY Acad. Sci. **1123,** 64–68 https://doi.org/10.1196/annals.1420.008

Colomer JM, Mao L, Rockman HA, Means AR (2003): Pressure overload selectively up-regulates Ca2+/calmodulin-dependent protein kinase II in vivo. Mol. Endocrinol. **17,** 183–192 https://doi.org/10.1210/me.2002-0350

Cooling MT, Hunter P, Crampin EJ (2009): Sensitivity of NFAT cycling to cytosolic calcium concentration: implications for hypertrophic signals in cardiac myocytes. Biophys. J. **96,** 2095–2104 https://doi.org/10.1016/j.bpj.2008.11.064

Cui J, Kaandorp JA (2008): Simulating Complex Calcium-Calcineurin Signaling Network. Paper presented at: International Conference on Computational Science (Springer) https://doi.org/10.1007/978-3-540-69389-5_14

Dai H, Jia G, Liu X, Liu Z, Wang H (2014): Astragalus polysaccharide inhibits isoprenaline-induced cardiac hypertrophy via suppressing Ca 2+-mediated calcineurin/NFATc3 and CaMKII signaling cascades. Environ. Toxicol. Pharmacol. **38,** 263–271 https://doi.org/10.1016/j.etap.2014.05.008

Despa S, Tucker AL, Bers DM (2008): Phospholemman-mediated activation of Na/K-ATPase limits [Na] i and inotropic state during β-adrenergic stimulation in mouse ventricular myocytes. Circulation **117,** 1849–1855
https://doi.org/10.1161/CIRCULATIONAHA.107.754051

Dolmetsch RE, Lewis RS, Goodnow CC, Healy JI (1997): Differential activation of transcription factors induced by Ca2+ response amplitude and duration. Nature **386,** 855–858
https://doi.org/10.1038/386855a0

Dolmetsch RE, Xu K, Lewis RS (1998): Calcium oscillations increase the efficiency and specificity of gene expression. Nature **392,** 933–936
https://doi.org/10.1038/31960

Dolmetsch R (2003): Excitation-transcription coupling: signaling by ion channels to the nucleus. Sci. STKE **2003,** PE4
https://doi.org/10.1126/stke.2003.166.pe4

Engelhardt S, Hein L, Wiesmann F, Lohse MJ (1999): Progressive hypertrophy and heart failure in β1-adrenergic receptor transgenic mice. Proc. Natl. Acad. Sci. USA **96,** 7059–7064
https://doi.org/10.1073/pnas.96.12.7059

Erickson JR, Patel R, Ferguson A, Bossuyt J, Bers DM (2011): Fluorescence resonance energy transfer–based sensor Camui provides new insight into mechanisms of calcium/calmodulin-dependent protein kinase II activation in intact cardiomyocytes. Circ. Res. **109,** 729–738
https://doi.org/10.1161/CIRCRESAHA.111.247148

Fearnley CJ, Roderick HL, Bootman MD (2011): Calcium signaling in cardiac myocytes. Cold Spring Harb. Perspect. Biol. **3,** a004242
https://doi.org/10.1101/cshperspect.a004242

Fisher WG, Yang PC, Medikonduri RK, Jafri MS (2006): NFAT and NFκB activation in T lymphocytes: a model of differential activation of gene expression. Ann. Biomed. Eng. **34,** 1712–1728
https://doi.org/10.1007/s10439-006-9179-4

Goonasekera SA, Molkentin JD (2012): Unraveling the secrets of a double life: contractile versus signaling Ca 2+ in a cardiac myocyte. J. Mol. Cell Cardiol. **52,** 317–322
https://doi.org/10.1016/j.yjmcc.2011.05.001

Grimm M, Brown JH (2010): β-Adrenergic receptor signaling in the heart: role of CaMKII. J. Mol. Cell. Cardiol. **48,** 322–330
https://doi.org/10.1016/j.yjmcc.2009.10.016

Gruver CL, DeMayo F, Goldstein MA, Means AR (1993): Targeted developmental overexpression of calmodulin induces proliferative and hypertrophic growth of cardiomyocytes in transgenic mice. Endocrinology **133,** 376–388
https://doi.org/10.1210/endo.133.1.8319584

Kang S (2013): Myocardial calcium signaling in physiology and disease. J. Receptor Ligand Channel Res. **6,** 1–13

Kang JH, Lee HS, Kang YW, Cho KH (2016): Systems biological approaches to the cardiac signaling network. Brief Bioinform. **17,** 419–428
https://doi.org/10.1093/bib/bbv039

Khalilimeybodi A, Daneshmehr A, Sharif-Kashani B (2017): Investigating β-adrenergic-induced cardiac hypertrophy through computational approach: classical and non-classical pathways. J. Physiol. Sci. (in press)
https://doi.org/10.1007/s12576-017-0557-5

Knollmann BC, Kirchhof P, Sirenko SG, Degen H, Greene AE, Schober T, Mackow JC, Fabritz L, Potter JD, Morad M (2003): Familial hypertrophic cardiomyopathy-linked mutant troponin T causes stress-induced ventricular tachycardia and Ca^{2+}-dependent action potential remodeling. Circ. Res. **92,** 428–436
https://doi.org/10.1161/01.RES.0000059562.91384.1A

Layland J, Kentish JC (1999): Positive force-and [Ca2+] i-frequency relationships in rat ventricular trabeculae at physiological frequencies. Am. J. Physiol. Heart Circ. Physiol. **276,** 9–18

Li C, Li X, Gao X, Zhang R, Zhang Y, Liang H, Xu C, Du W, Zhang Y, Liu X (2014): MicroRNA-328 as a regulator of cardiac hypertrophy. Int. J. Cardiol. **173,** 268–276
https://doi.org/10.1016/j.ijcard.2014.02.035

Liu N, Denegri M, Ruan Y, Avelino-Cruz JE, Perissi A, Negri S, Napolitano C, Coetzee WA, Boyden PA. Priori SG (2011): Flecainide exerts an antiarrhythmic effect in a mouse model of catecholaminergic polymorphic ventricular tachycardia by increasing the threshold for triggered activity. Circ. Res. **109,** 291–295
https://doi.org/10.1161/CIRCRESAHA.111.247338

Mattiazzi A, Bassani RA, Escobar AL, Palomeque J, Valverde CA, Petroff MV, Bers DM (2015): Chasing cardiac physiology and pathology down the CaMKII cascade. Am. J. Physiol. Heart Circ. Physiol. **308,** 1177–1191
https://doi.org/10.1152/ajpheart.00007.2015

Molkentin JD (2004): Calcineurin–NFAT signaling regulates the cardiac hypertrophic response in coordination with the MAPKs. Cardiovasc. Res. **63,** 467–475
https://doi.org/10.1016/j.cardiores.2004.01.021

Molkentin JD (2006): Dichotomy of Ca 2+ in the heart: contraction versus intracellular signaling. J. Clin. Invest. **116,** 623–626
https://doi.org/10.1172/JCI27824

O'Keefe SJ, Tamura J, Kincaid RL, Tocci MJ, O'Neill EA (1992): FK-506-and CsA-sensitive activation of the interleukin-2 promoter by calcineurin. Nature **357,** 692–694
https://doi.org/10.1038/357692a0

Onal B, Unudurthi SD, Hund TJ (2014): Modeling CaMKII in cardiac physiology: from molecule to tissue. Front. Pharmacol. **5,** 9
https://doi.org/10.3389/fphar.2014.00009

Pall GS, Johnson KJ, Smith GL (2003): Abnormal contractile activity and calcium cycling in cardiac myocytes isolated from DMPK knockout mice. Physiol. Genomics **13,** 139–146
https://doi.org/10.1152/physiolgenomics.00107.2002

Roderick HL, Higazi D, Smyrnias I, Fearnley C, Harzheim D, Bootman M (2007): Calcium in the heart: when it's good, it's very very good, but when it's bad, it's horrid. Biochem. Soc. Trans. **35,** 957–961
https://doi.org/10.1042/BST0350957

Sanna B, Bueno OF, Dai YS, Wilkins BJ, Molkentin JD (2005): Direct and indirect interactions between calcineurin-NFAT and MEK1-extracellular signal-regulated kinase 1/2 signaling pathways regulate cardiac gene expression and cellular growth. Mol. Cell. Biol. **25,** 865–878
https://doi.org/10.1128/MCB.25.3.865-878.2005

Saucerman JJ, McCulloch AD (2006): Cardiac β-Adrenergic Signaling. Ann. NY Acad. Sci. **1080,** 348–361
https://doi.org/10.1196/annals.1380.026

Saucerman JJ, Bers DM (2008): Calmodulin mediates differential sensitivity of CaMKII and calcineurin to local Ca 2+ in cardiac myocytes. Biophys. J. **95,** 4597–4612
https://doi.org/10.1529/biophysj.108.128728

Shen T, Cseresnyés Z, Liu Y, Randall WR, Schneider MF (2007): Regulation of the nuclear export of the transcription factor NFATc1 by protein kinases after slow fibre type electrical stimulation of adult mouse skeletal muscle fibres. J. Physiol. **579,** 535–551
https://doi.org/10.1113/jphysiol.2006.120048

Shin SY, Choo SM, Kim D, Baek SJ, Wolkenhauer O, Cho KH (2006): Switching feedback mechanisms realize the dual role of MCIP in the regulation of calcineurin activity. FEBS Lett **580,** 5965–5973
https://doi.org/10.1016/j.febslet.2006.09.064

Shin SY, Yang JM, Choo SM, Kwon KS, Cho KH (2008): System-level investigation into the regulatory mechanism of the calcineurin/NFAT signaling pathway. Cell Signal. **20,** 1117–1124
https://doi.org/10.1016/j.cellsig.2008.01.023

Shin SY, Yang HW, Kim JR, Do Heo W, Cho KH (2011): A hidden incoherent switch regulates RCAN1 in the calcineurin–NFAT signaling network. J. Cell. Sci. **124,** 82–90
https://doi.org/10.1242/jcs.076034

Song Q, Saucerman JJ, Bossuyt J, Bers DM (2008): Differential integration of Ca2+-calmodulin signal in intact ventricular myocytes at low and high affinity Ca2+-calmodulin targets. J. Biol. Chem. **283,** 31531–31540
https://doi.org/10.1074/jbc.M804902200

Song J, Gao E, Wang J, Zhang XQ, Chan TO, Koch WJ, Shang X, Joseph JI, Peterson BZ, Feldman AM (2012): Constitutive overexpression of phosphomimetic phospholemman S68E mutant results in arrhythmias, early mortality, and heart failure: potential involvement of Na+/Ca2+ exchanger. Am. J. Physiol. Heart Circ. Physiol. **302,** 770–781
https://doi.org/10.1152/ajpheart.00733.2011

Stemmer PM, Klee CB (1994): Dual calcium ion regulation of calcineurin by calmodulin and calcineurin B. Biochemistry **33,** 6859–6866
https://doi.org/10.1021/bi00188a015

Tavi P, Pikkarainen S, Ronkainen J, Niemelä P, Ilves M, Weckström M, Vuolteenaho O, Bruton J, Westerblad H, Ruskoaho H (2004): Pacing-induced calcineurin activation controls cardiac Ca2+ signalling and gene expression. J. Physiol. **554,** 309–320
https://doi.org/10.1113/jphysiol.2003.053579

Tomida T, Hirose K, Takizawa A, Shibasaki F, Iino M (2003): NFAT functions as a working memory of Ca2+ signals in decoding Ca2+ oscillation. EMBO J. **22,** 3825–3832
https://doi.org/10.1093/emboj/cdg381

Vinogradova TM, Bogdanov KY, Lakatta EG (2002): β-Adrenergic stimulation modulates ryanodine receptor Ca2+ release during diastolic depolarization to accelerate pacemaker activity in rabbit sinoatrial nodal cells. Circ. Res. **90,** 73–79
https://doi.org/10.1161/hh0102.102271

Wang H, Kohr MJ, Wheeler DG, Ziolo MT (2008): Endothelial nitric oxide synthase decreases β-adrenergic responsiveness via inhibition of the L-type Ca2+ current. Am. J. Physiol. Heart Circ. Physiol. **294,** H1473–H1480
https://doi.org/10.1152/ajprenal.00036.2008

Wilkins BJ, Molkentin JD (2004): Calcium–calcineurin signaling in the regulation of cardiac hypertrophy. Biochem. Biophys. Res. Commun. **322,** 1178–1191
https://doi.org/10.1016/j.bbrc.2004.07.121

Winslow RL, Walker MA, Greenstein JL (2016): Modeling calcium regulation of contraction, energetics, signaling, and transcription in the cardiac myocyte. Wiley Interdiscip. Rev. Syst. Biol. Med. **8,** 37–67
https://doi.org/10.1002/wsbm.1322

Xia Y, McMillin JB, Lewis A, Moore M, Zhu WG, Williams RS, Kellems RE (2000): Electrical stimulation of neonatal cardiac myocytes activates the NFAT3 and GATA4 pathways and upregulates the adenylosuccinate synthetase 1 gene. J. Biol. Chem. **275,** 1855–1863
https://doi.org/10.1074/jbc.275.3.1855

Yang JH, Saucerman JJ (2011): Computational models reduce complexity and accelerate insight into cardiac signaling networks. Circ. Res. **108,** 85–97
https://doi.org/10.1161/CIRCRESAHA.110.223602

Zhang T, Brown JH (2004): Role of Ca2+/calmodulin-dependent protein kinase II in cardiac hypertrophy and heart failure. Cardiovasc. Res. **63,** 476–486
https://doi.org/10.1016/j.cardiores.2004.04.026

Zou Y, Yao A, Zhu W, Kudoh S, Hiroi Y, Shimoyama M, Uozumi H, Kohmoto O, Takahashi T, Shibasaki F, Nagai R. (2001): Isoproterenol activates extracellular signal–regulated protein kinases in cardiomyocytes through calcineurin. Circulation **104,** 102–108
https://doi.org/10.1161/hc2601.090987

Received: February 16, 2017
Final version accepted: June 16, 2017

doi: 10.4149/gpb_2017022

Supplementary Material

Ca^{2+}-dependent calcineurin/NFAT signaling in β-adrenergic-induced cardiac hypertrophy

Ali Khalilimeybodi[1], Alireza Daneshmehr[1] and Babak Sharif Kashani[2]

[1] *Department of Mechanical Engineering, College of Engineering, University of Tehran, Tehran, Iran*
[2] *Department of Cardiology, Massih-Daneshvari Hospital, Shahid Beheshti University of Medical Sciences, Tehran, Iran*

1. Model description

1.1. β-adrenergic signaling model

In the β-adrenergic classical signaling, β-ARs stimulation by agonist results in the activation of Gs proteins. Activated Gs proteins stimulate adenylyl cyclase (AC) which subsequently activates cyclic AMP (cAMP). The raised level of cAMP stimulates PKA and leads to the PKA substrates phosphorylation. In parallel with classical pathway, PKA-mediated coupling of β2-AR to Gi proteins activates β-adrenergic non-classical pathways involving PI3K/Akt/GSK3β and Src/Ras/Raf/MEK/ERK. In the PI3K/Akt/GSK3β pathway, promotion of PI3K kinase activity by Gi leads to production of phosphatidylinositol-3,4,5-trisphosphate (PIP3) and subsequent Akt activation through phosphorylation on Thr^{308} and Ser^{473}. Fully activated Akt phosphorylates $GSK3\beta_c$ and attenuates its kinase activity. Among the β-adrenergic pathways, direct and indirect impacts of AC/cAMP/PKA and PI3K/Akt/GSK3β pathways components on calcineurin/NFAT signaling have been established (Shin et al. 2011; Wilkins and Molkentin 2004).

The main intracellular kinase acts as a downstream of Gi subunits in ISO-induced ERK1/2 activation is tyrosine kinase Src (Ma et al., 2000). Gi_α proteins directly stimulate Src activity, but for $Gi_{\beta\gamma}$ proteins, it is reported that $Gi_{\beta\gamma}$ subunit activates Src through PI3K (Luttrell et al., 1996). In the activation of ERK1/2 by β2-AR, activated Src phosphorylates Shc adaptor protein. Then, phosphorylated Shc recruits the growth factor receptor-binding protein 2 (Grb2) and Son of Sevenless homologue protein (Sos) to form Shc-Grb2-Sos complex. Also, phosphorylated Shc could bind with Grb2-Sos (GS) complex to form Shc-Grb2-Sos. Shc-Grb2-Sos complex activates Ras by enhancement of GDP–GTP exchange on Ras proteins through guanine nucleotide exchange factor Sos (Zou et al., 1999). In ERK1/2 signaling, activated Ras induces activation of Raf via phosphorylation. Activated Raf acts as MEK kinase and catalyzes activation of MEK by its phosphorylation on defined serine/threonine residues. On the other hand, PP2A deactivates the MEK by its dephosphorylation. Double phosphorylated MEK (MEKPP) phosphorylates and activates ERK1/2. Also, MAPK phosphatase 3 (MKP3) negatively regulates MAP kinases (ERK1/2) by double dephosphorylation of ERKPP (Hatakeyama et al., 2003). For Src/Ras/Raf/MEK/ERK pathway, although there are evidences on the cross-talks with calcineurin/NFAT pathway in β-AR-induced cardiac hypertrophy (Zou et al., 2001), Sanna et al. (2005) found that these interactions are independent of calcineurin and changes in NFAT nuclear localization and mainly origin from NFAT associations with GATA4 and Activator protein 1 (AP-1) transcription factors which is not in our study scope.

In addition to the cytosolic components of β-adrenergic signaling including cyclic AMP (cAMP), PKA_c, Akt and $GSK3\beta_c$ which their ISO-induced variations are shown in Fig S1, it is found that nuclear kinases such as $GSK3\beta_n$ and PKA_n contribute in $NFAT_n$ phosphorylation and promote its nuclear export (Wilkins and Molkentin, 2004). So, to consider the nucleocytoplasmic shuttling of PKA and GSK3β in our model, we assume that PKA catalytic subunits diffuse slowly into the nucleus after β-AR stimulation. Our assumption is based on the Yang et al. (2014) study which showed that in β-adrenergic signaling, slow diffusion of PKA catalytic subunits results in the differences in cytosolic and nuclear PKA dynamics. For GSK3β, Morisco et al. (2001) demonstrated that ISO stimulation leads to the nuclear export of GSK3β. Also, it is found that GSK3β can be localized to the cytosol or the nucleus and PI3K signaling promotes its nuclear export (Shin et al., 2011). So, we assume that β-AR-induced Akt activation enhances GSK3β nuclear export and GSK3β is mainly localized to the cytosol in unstimulated cells (Shin et al., 2011).

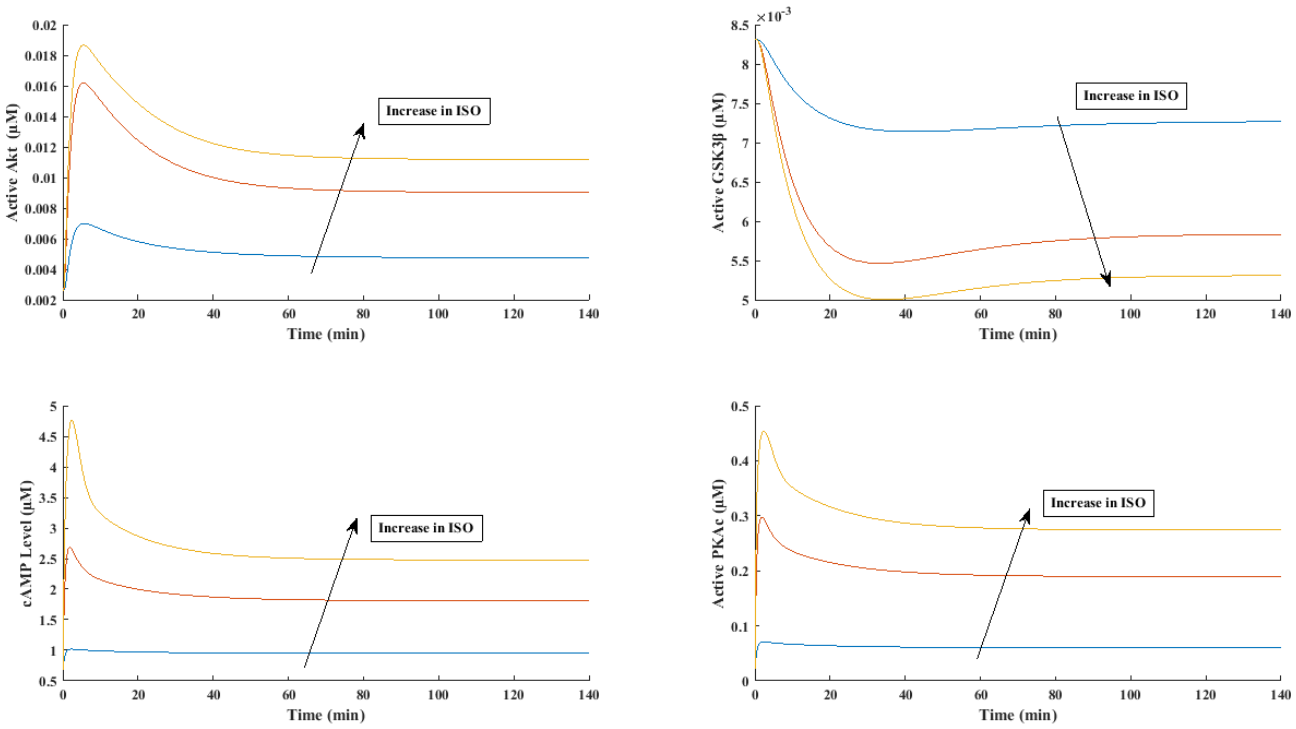

Figure S1. The ISO-induced time courses of four main cytosolic components of β-adrenergic signaling. The diagrams were obtained through our previous model for different ISO concentration (10 nM, 100 nM, 1 μM).

1.2. Ca^{2+} model

In general, intracellular free calcium level in cardiac myocytes varies beat-to-beat in the range of 0.1–1 μM and isoproterenol infusion alters its amplitude and frequency. In this regard, It has been shown that cardiomyocytes stimulation by isoproterenol increases the heart beating rate and leads to a rapid and marked elevation in systolic and diastolic levels of intracellular calcium (Zou et al., 2001). However, the detailed mechanism of this elevation is complicated and depends on many factors. In a PKA-dependent mechanism during β-AR stimulation, phosphorylation of L-type Ca^{2+} channels (LTCCs), phospholamban (PLB), and ryanodine receptors (RyRs) by PKA results in a rapid elevation in cytoplasmic Ca^{2+} (Bers, 2001; Xiang and Kobilka, 2003). Moreover, there exist PKA-independent pathways which mediate β-adrenergic effects on Ca^{2+} transient such as cAMP/Epac/CaMKII pathway (Grimm and Brown, 2010). It is found that elevation of cAMP level after β-AR stimulation is adequate to activate Epac and its activation reduces the amplitude of the cytoplasmic Ca^{2+} transient and increases its decay time through RyRs phosphorylation via CaMKII (Pereira et al., 2007; Pereira et al., 2012). In addition to the cytosolic Ca^{2+} transient, nuclear Ca^{2+} transient could also be a mediator for transducing hypertrophic signals. It is established that nuclear Ca^{2+} follows cytosolic Ca^{2+} transient in each oscillation due to the rapid passive diffusion of Ca^{2+} through nuclear pore complexes (NPCs) and its amplitude is smaller than cytosolic Ca^{2+} transient and also declines slower than cytosolic Ca^{2+} transient (Ljubojević et al., 2011). In the signaling pathways which IP3 receptors are activated, nuclear Ca^{2+} transient plays a great role in hypertrophy. But in the β-adrenergic stimulation by ISO, IP3 activation is not a noticeable contributing factor and as Cooling et al. (2009) showed that activated NFAT sensitivity to nuclear Ca^{2+} transient is not significant. Thus, we neglect the effects of nuclear Ca^{2+} transient on NFAT signaling in our study.

In this study, for the sake of simplicity, we model the Ca^{2+} transient in the cardiomyocytes based on the hypothetical calcium model presented by Negroni and Lascano (1996). We modified this model to take into account important phenomena such as frequency dependence of Ca^{2+} transient characteristics including diastolic and systolic levels, peak time, half-width and decay time constant, and the effects of β-AR stimulation on the amplitude and frequency of Ca^{2+} transient. Since the detailed mechanism of cAMP and PKA effects on Ca^{2+} transient is complex and

ISO-induced PKA dynamics is dependent and similar to cAMP dynamics, we modified the basic model by adding a cAMP level-dependent term to include β-ARs stimulation effects in our model. We calibrate the adding term's parameter to obtain ISO-induced Ca^{2+} transient amplitude in the range of experimental results. The other calcium model parameters are obtained directly from the literature or estimated from experimental data.

1.3. Calcineurin model

Alterations in intracellular calcium concentration usually affect downstream pathways through Ca^{2+}-binding proteins. Calmodulin (CaM) is a ubiquitous Ca^{2+}-binding protein which mediates diverse cellular events such as hypertrophic growth of cardiomyocytes (Zou et al., 2001). Calmodulin binds four calcium ions. The two of them bind to the C-terminal EF hand and afterwards two bind to the N-terminal EF hand. This sequence is due to the higher Ca^{2+} affinity for sites in the C-terminal domain than those in the N-terminal domain (Linse et al., 1991; Saucerman and Bers, 2008). Ca^{2+}-saturated calmodulin (CaMCa4) binds to calcineurin at exceptionally high affinity and activates it (Quintana et al., 2005). Activated calcineurin could shuttle between cytosol and nucleus and dephosphorylate signaling components including NFAT proteins in both compartments (Shibasaki et al., 1996).

Since the dissociation rate of calcium ions from C-terminal domain ($10\ s^{-1}$) is slower than N-terminal domain ($500\ s^{-1}$) (Klee, 1988), it is possible that the variation in calcium transient frequency affects the fraction of C- and N-terminal occupancy by calcium ions and consequently alters CaN activity (Chiba et al., 2008). So, we use a sequential four-step Ca^{2+} binding model for calmodulin activation based on the model presented by Holmes (2000). The model considers Ca^{2+} cooperative binding within each domain and the sequence of Ca^{2+} binding to the C-terminal and N-terminal sites. The model parameters is obtained from previous studies or estimated to fit experimental data on CaN activity (Stemmer and Klee, 1994). The rate of Ca^{2+}/CaM association and dissociation from calcineurin is obtained from Quintana et al. (2005) study with $K_d = 28$ pM. Also, the rate of active calcineurin import and export from the nucleus is determined from Shibasaki et al. (1996) study on calcineurin/NFAT nuclear shuttling.

1.4. NFAT model

Nuclear factor of activated T cells (NFAT) is a key transcription factor that integrates intracellular Ca^{2+} signals and hypertrophic genes expression. There exist four NFAT isoforms ($NFAT_c1$-4) in the mammalian hearts which are regulated by Ca^{2+}-dependent calcineurin activation (Rinne et al., 2010). In unstimulated cells, $NFAT_c$ factors are usually localized to the cytoplasm in a phosphorylated state. Calcineurin dephosphorylates NFAT which results in the unmasking of nuclear localization signals (NLS) and, consequently, translocation of NFAT proteins to the nucleus. On the other hand, protein kinases such as GSK3β, and PKA phosphorylate $NFAT_c$ and antagonize calcineurin phosphatase activity and $NFAT_c$ nuclear import. NFAT translocation to the nucleus activates the transcription of downstream targets. In the nucleus, although nuclear kinases such as PKA_n and $GSK3\beta_n$ phosphorylate free nuclear $NFAT_n$ and stimulate its nuclear export through exposing a nuclear export signal domain, activated calcineurin in the nucleus (CaN_n) resists against the $NFAT_n$ phosphorylation by kinases and tries to maintain the nuclear $NFAT_n$ transcriptional activity (Wilkins and Molkentin, 2004).

In our NFAT model, in the initial state, all of NFAT proteins are phosphorylated and localized in the cytoplasm. The dephosphorylation of $NFAT_c$ by active calcineurin and its rephosphorylation by PKA_c and $GSK3\beta_c$ are described by Michaelis–Menten kinetic model. We use the same model for the phosphorylation of $NFAT_n$ by nuclear kinases PKA_n and $GSK3\beta_n$ and its dephosphorylation by nuclear active calcineurin (CaN_n) in the nucleus. The NFAT nuclear import and export use the Ran cycle and hence are considered irreversible in our model (Cooling et al., 2009). The rates of NFAT nuclear import and export are obtained directly from Shibasaki et al. (1996) study. Also, according to the Shin et al. (2006) study, the expression of MCIP1 under ISO infusion is negligible and MCIP1 hardly inhibits active calcineurin. Therefore, we do not consider NFAT-mediated MCIP1 expression and its regulatory effect on calcineurin activation in our model. The model parameters are estimated by fitting the simulation results to the experimental nuclear NFAT transients in excitable cells (Shen et al., 2007).

Model parameters:

Table S1. Model state variables

State Variables	Description	Initial with constant Ca^{2+} (μM)	Initial with 1Hz oscillatory Ca^{2+} (μM)
Ca^{2+}	Concentration of free calcium	1.700 E-01	1.700 E-01
CaM_f	Concentration of free CaM	5.943E+0	5.916E+0
$CaMCa$	Concentration of CaMCa	3.536 E-02	3.565 E-02
$CaMCa_2$	Concentration of CaMCa2	7.012 E-03	7.218 E-03
$CaMCa_3$	Concentration of CaMCa3	1.190 E-05	1.236 E-05
$CaMCa_4$	Concentration of CaMCa4	4.050 E-07	4.817 E-07
CaN_c	Concentration of cytosolic inactive CaN	9.853 E-01	9.587 E-01
CaN_c^*	Concentration of cytosolic active CaN	1.413 E-02	3.969 E-02
CaN_n^*	Concentration of nuclear active CaN	2.918 E-02	8.200 E-02
$NFAT_{cp}$	Concentration of phosphorylated cytosolic NFAT	1.617 E-02	1.281 E-02
$NFAT_c$	Concentration of dephosphorylated cytosolic NFAT	1.170 E-04	2.726 E-04
$NFAT_n$	Concentration of dephosphorylated nuclear NFAT	3.542 E-02	1.957 E-01
$NFAT_{np}$	Concentration of phosphorylated nuclear NFAT	1.880 E-04	4.367 E-04
PKA_n	Concentration of PKA catalytic subunit in nucleus	2.177 E-02	2.177 E-02
$GSK3\beta_n$	Concentration of GSK3β in nucleus	1.737 E-03	1.737 E-03

Table S2. Model parameters and protein concentrations

Parameter	Value	Unit	Source
CaM_{tot}	6.0*	(μM)	(Fabiato, 1983; Maier and Bers, 2002)
CaN_{tot}	1.0*	(μM)	(Bhalla and Iyengar, 1999; Shin et al., 2006)
$NFAT_{tot}$	1.7 E-02*	(μM)	(Arron et al., 2006; Shin et al., 2006)
K_{nuc}	50.0*		(Bers, 2001)
K_{1dia}	3.0 E-02†	(s. μM)	(Pall et al., 2003)
K_{2dia}	1.4 E-01†	(μM)	(Pall et al., 2003)
$K_{C_{KP}}$	1.4 E+01†	($\mu M.s^{-0.5}$)	(Pall et al., 2003)
$n_{C_{KP}}$	5.0 E-01 †		(Pall et al., 2003)
K_m	8.0 E-01†	(μM)	(Pall et al., 2003)
$K_{Q_m:cAMP}$	5.0†		(Adjusted to be in experimental results range)
K_{Q_m}	1.1 E+01†	($\mu M.s^{-0.67}$)	(Pall et al., 2003)
n_{Q_m}	3.3 E-01†		(Pall et al., 2003)
T_p	2.5 E-02*	(s)	(Negroni and Lascano, 1996)
K_{CaM+1}	3.5 E-01†	($\mu M^{-1}.s^{-1}$)	(Stemmer and Klee, 1994)
K_{CaM-1}	1.0 E+01*	(s^{-1})	(Klee, 1988)
K_{CaM+2}	33.33∗ K_{CaM+1}*	($\mu M^{-1}.s^{-1}$)	(Holmes, 2000)
K_{CaM-2}	1.0 E+01*	(s^{-1})	(Klee, 1988)
K_{CaM+3}	5.0*	($\mu M^{-1}.s^{-1}$)	(Holmes, 2000)
K_{CaM-3}	5.0 E+02*	(s^{-1})	(Klee, 1988)
K_{CaM+4}	1.0 E+02*	($\mu M^{-1}.s^{-1}$)	(Holmes, 2000)
K_{CaM-4}	5.0 E+02*	(s^{-1})	(Klee, 1988)
K_{CaN+1}	4.6 E+01*	($\mu M^{-1}.s^{-1}$)	(Quintana et al., 2005)
K_{CaN-1}	1.3 E-03*	(s^{-1})	(Quintana et al., 2005)
K_{CaN+2}	1.9 E-03*	(s^{-1})	(Shibasaki et al., 1996)
K_{CaN-2}	9.2 E-04*	(s^{-1})	(Shibasaki et al., 1996)
K_{N1}	1.19 E-04*	(s^{-1})	(Yang et al., 2014)
K_{N+2}	8.8977 E-06†	(s^{-1})	(Shin et al., 2011)
$K_{N-2.1}$	9.0 E-06†	(s^{-1})	(Shin et al., 2011)
$K_{N-2.2}$	1.287 E-02†	($\mu M^{-1}.s^{-1}$)	(Shin et al., 2011)
K_{N3}	1.54 E-03*	(s^{-1})	(Shibasaki et al., 1996)
K_{N4}	9.6 E-04*	(s^{-1})	(Shibasaki et al., 1996)
K_{N+5}. K_{N+6}	5.0 E-01†	(s^{-1})	(Shen et al., 2007)
K_{N+5m}. K_{N+6m}	1.0 E-01†	(μM)	(Shen et al., 2007)
$K_{N-5.1}$. $K_{N-6.1}$	1.0 E-01†	(s^{-1})	(Shen et al., 2007)
$K_{N-5.2}$. $K_{N-6.2}$	1.0 E+01†	(s^{-1})	(Shen et al., 2007)
K_{N-5m}	1.0 E-02†	(μM)	(Shen et al., 2007)
K_{N-6m}	1.9 E+01†	(μM)	(Shen et al., 2007)
K_{Gi}	4.5 E-04†	(s^{-1})	(Shen et al., 2007)
K_{Ci}	7.7 E-04*	(s^{-1})	(Halloran et al., 1999)

†: Estimated *: directly obtained

3. Model Equations

Ca^{2+} Module

$$Ca^{2+}_{dia} = K_{1dia}.Hz + K_{2dia} \quad (A.1)$$

$$C_{KP} = \left(\frac{[cAMP] - [cAMP_{int}]}{1 + [cAMP]} + 1\right).K_{C_{KP}}.(Hz)^{n_{C_{KP}}} \quad (A.2)$$

$$C_{QP_{rest}} = \frac{C_{KP}}{1 + \left(\frac{K_m}{Ca^{2+}_{dia}}\right)^2} \quad (A.3)$$

$$Q_m = K_{Q_m:cAMP}.\left(\frac{[cAMP]-[cAMP_{int}]}{1+[cAMP]} + 1\right).K_{Q_m}.(Hz)^{n_{Q_m}} \quad (A.4)$$

$$Q_{pump} = \frac{C_{KP}}{1 + \left(\frac{K_m}{[Ca^{2+}]}\right)^2} \quad (A.5)$$

$$T_f = t - \frac{floor(t.Hz)}{Hz} \quad (A.6)$$

$$Q_{rel} = Q_m.\left(\frac{T_f}{T_p}\right)^4.e^{4\left(1-\frac{T_f}{T_p}\right)} + C_{QP_{rest}} \quad (A.7)$$

$$\frac{d[Ca^{2+}]}{dt} = Q_{rel} - Q_{pump} \quad (A.8)$$

$$Hz_{ISO} = 1 + \frac{0.4}{1+\left(\frac{0.105}{[ISO]}\right)^{1.5}} \quad (A.9)$$

CaN Module

$$CaM1 = K_{CaM+1}.[Ca^{2+}].[CaM_f] - K_{CaM-1}.[CaMCa] \quad (A.10)$$

$$CaM2 = K_{CaM+2}.[Ca^{2+}].[CaMCa] - K_{CaM-2}.[CaMCa_2] \quad (A.11)$$

$$CaM3 = K_{CaM+3}.[Ca^{2+}].[CaMCa_2] - K_{CaM-3}.[CaMCa_3] \quad (A.12)$$

$$CaM4 = K_{CaM+4}.[Ca^{2+}].[CaMCa_3] - K_{CaM-4}.[CaMCa_4] \quad (A.13)$$

$$CaN1 = K_{CaN+1}.[CaMCa_4].[CaN_c] - K_{CaN-1}.[CaN^*_c] \quad (A.14)$$

$$CaN2 = K_{CaN+2}.[CaN^*_c] - K_{CaN-2}.[CaN^*_n] \quad (A.15)$$

$$\frac{d[CaM_f]}{dt} = -CaM1 \quad (A.16)$$

$$\frac{d[CaMCa]}{dt} = CaM1 - CaM2 \quad (A.17)$$

$$\frac{d[CaMCa_2]}{dt} = CaM2 - CaM3 \quad (A.18)$$

$$\frac{d[CaMCa_3]}{dt} = CaM3 - CaM4 \quad (A.19)$$

$$\frac{d[CaMCa_4]}{dt} = CaM4 - CaN1 \quad (A.20)$$

$$\frac{d[CaN_c]}{dt} = -CaN1 \quad (A.21)$$

$$\frac{d[CaN^*_c]}{dt} = CaN1 - CaN2 \quad (A.22)$$

$$\frac{d[CaN^*_n]}{dt} = K_{nuc}.CaN2 \quad (A.23)$$

NFAT Module

$$N1 = K_{N1}.([PKA_c] - [PKA_n]) \quad (A.24)$$

$$N2 = K_{N+2}.[GSK3\beta_c] - (K_{N-2.1} + K_{N-2.2}[Akt_{pp}]).[GSK3\beta_n] \quad (A.25)$$

$$N3 = K_{N3}.[NFAT_c] \quad (A.26)$$

$$N4 = K_{N4}.[NFAT_{np}] \quad (A.27)$$

$$N5 = \frac{K_{N+5}.[CaN_c^*].[NFAT_{cp}]}{K_{N+5m} + [NFAT_{cp}]} - \frac{(K_{N-5.1}.[PKA_c] + K_{N-5.2}.[GSK3\beta_c]).[NFAT_c]}{K_{N-5m} + [NFAT_c]} \quad (A.28)$$

$$N6 = \frac{K_{N+6}.[CaN_n^*].[NFAT_{np}]}{K_{N+6m} + [NFAT_{np}]} - \frac{(K_{N-6.1}.[PKA_n] + K_{N-6.2}.[GSK3\beta_n]).[NFAT_n]}{K_{N-6m} + [NFAT_n]} \quad (A.29)$$

$$\frac{d[NFAT_{cp}]}{dt} = -N5 + N4 \quad (A.30)$$

$$\frac{d[NFAT_c]}{dt} = N5 - N3 \quad (A.31)$$

$$\frac{d[NFAT_n]}{dt} = K_{nuc}.N3 + N6 \quad (A.32)$$

$$\frac{d[NFAT_{np}]}{dt} = -K_{nuc}.N4 - N6 \quad (A.33)$$

$$\frac{d[PKA_n]}{dt} = K_{nuc}.N1 \quad (A.34)$$

$$\frac{d[GSK3\beta_n]}{dt} = K_{nuc}.N2 \quad (A.35)$$

$$GSK3\beta_{inhibition} = K_{Gi}.[GSK3\beta_c] \quad (A.36)$$

$$CaN_{inhibition} = K_{Ci}.[CaN_c^*] \quad (A.37)$$

References

Arron, J.R., Winslow, M.M., Polleri, A., Chang, C.-P., Wu, H., Gao, X., Neilson, J.R., Chen, L., Heit, J.J., and Kim, S.K. (2006). NFAT dysregulation by increased dosage of DSCR1 and DYRK1A on chromosome 21. Nature **441,** 595-600. https://doi.org/10.1038/nature04678

Bers, D. (2001). Excitation-contraction coupling and cardiac contractile force, Vol 237 (Springer Science & Business Media). https://doi.org/10.1007/978-94-010-0658-3

Bhalla, U.S., and Iyengar, R. (1999). Emergent properties of networks of biological signaling pathways. Science **283,** 381-387. https://doi.org/10.1126/science.283.5400.381

Chiba, H., Schneider, N.S., Matsuoka, S., and Noma, A. (2008). A simulation study on the activation of cardiac CaMKII δ-isoform and its regulation by phosphatases. Biophysical journal **95,** 2139-2149. https://doi.org/10.1529/biophysj.107.118505

Cooling, M.T., Hunter, P., and Crampin, E.J. (2009). Sensitivity of NFAT cycling to cytosolic calcium concentration: implications for hypertrophic signals in cardiac myocytes. Biophysical journal **96,** 2095-2104. https://doi.org/10.1016/j.bpj.2008.11.064

Fabiato, A. (1983). Calcium-induced release of calcium from the cardiac sarcoplasmic reticulum. American Journal of Physiology-Cell Physiology **245,** C1-C14.

Grimm, M., and Brown, J.H. (2010). β-Adrenergic receptor signaling in the heart: role of CaMKII. Journal of molecular and cellular cardiology **48,** 322-330. https://doi.org/10.1016/j.yjmcc.2009.10.016

Halloran, P.F., Helms, L.M., Kung, L., and Noujaim, J. (1999). THE TEMPORAL PROFILE OF CALCINEURIN INHIBITION BY CYCLOSPORINE IN VIVO1. Transplantation **68,** 1356-1361. https://doi.org/10.1097/00007890-199911150-00023

Hatakeyama, M., Kimura, S., Takashi, N., Kawasaki, T., Yumoto, N., Ichikawa, M., Jae-Hoon, K., Saito, K., Saeki, M., and Shirouzu, M. (2003). A computational model on the modulation of mitogen-activated protein kinase (MAPK) and Akt pathways in heregulin-induced ErbB signalling. Biochemical Journal **373,** 451-463. https://doi.org/10.1042/bj20021824

Holmes, W.R. (2000). Models of calmodulin trapping and CaM kinase II activation in a dendritic spine. Journal of computational neuroscience **8,** 65-86. https://doi.org/10.1023/A:1008969032563

Klee, C.B. (1988). Interaction of calmodulin with Ca2+ and target proteins. Calmodulin **5,** 35-56.

Linse, S., Helmersson, A., and Forsen, S. (1991). Calcium binding to calmodulin and its globular domains. Journal of Biological Chemistry **266,** 8050-8054.

Ljubojević, S., Walther, S., Asgarzoei, M., Sedej, S., Pieske, B., and Kockskämper, J. (2011). In situ calibration of nucleoplasmic versus cytoplasmic Ca 2+ concentration in adult cardiomyocytes. Biophysical journal **100,** 2356-2366. https://doi.org/10.1016/j.bpj.2011.03.060

Luttrell, L.M., Hawes, B.E., van Biesen, T., Luttrell, D.K., Lansing, T.J., and Lefkowitz, R.J. (1996). Role of c-Src tyrosine kinase in G protein-coupled receptorand Gβγ subunit-mediated activation of mitogen-activated protein kinases. Journal of Biological Chemistry **271,** 19443-19450.

https://doi.org/10.1074/jbc.271.32.19443
Ma, Y.-C., Huang, J., Ali, S., Lowry, W., and Huang, X.-Y. (2000). Src tyrosine kinase is a novel direct effector of G proteins. Cell **102,** 635-646. https://doi.org/10.1016/S0092-8674(00)00086-6
Maier, L.S., and Bers, D.M. (2002). Calcium, calmodulin, and calcium-calmodulin kinase II: heartbeat to heartbeat and beyond. Journal of molecular and cellular cardiology **34,** 919-939. https://doi.org/10.1006/jmcc.2002.2038
Morisco, C., Seta, K., Hardt, S.E., Lee, Y., Vatner, S.F., and Sadoshima, J. (2001). Glycogen synthase kinase 3β regulates GATA4 in cardiac myocytes. Journal of Biological Chemistry **276,** 28586-28597. https://doi.org/10.1074/jbc.M103166200
Negroni, J.A., and Lascano, E.C. (1996). A cardiac muscle model relating sarcomere dynamics to calcium kinetics. Journal of molecular and cellular cardiology **28,** 915-929. https://doi.org/10.1006/jmcc.1996.0086
Pall, G.S., Johnson, K.J., and Smith, G.L. (2003). Abnormal contractile activity and calcium cycling in cardiac myocytes isolated from DMPK knockout mice. Physiological genomics **13,** 139-146. https://doi.org/10.1152/physiolgenomics.00107.2002
Pereira, L., Métrich, M., Fernández-Velasco, M., Lucas, A., Leroy, J., Perrier, R., Morel, E., Fischmeister, R., Richard, S., and Bénitah, J.P. (2007). The cAMP binding protein Epac modulates Ca2+ sparks by a Ca2+/calmodulin kinase signalling pathway in rat cardiac myocytes. The Journal of physiology **583,** 685-694. https://doi.org/10.1113/jphysiol.2007.133066
Pereira, L., Ruiz-Hurtado, G., Morel, E., Laurent, A.-C., Métrich, M., Domínguez-Rodríguez, A., Lauton-Santos, S., Lucas, A., Benitah, J.-P., and Bers, D.M. (2012). Epac enhances excitation–transcription coupling in cardiac myocytes. Journal of molecular and cellular cardiology **52,** 283-291. https://doi.org/10.1016/j.yjmcc.2011.10.016
Quintana, A.R., Wang, D., Forbes, J.E., and Waxham, M.N. (2005). Kinetics of calmodulin binding to calcineurin. Biochemical and biophysical research communications **334,** 674-680. https://doi.org/10.1016/j.bbrc.2005.06.152
Rinne, A., Kapur, N., Molkentin, J.D., Pogwizd, S.M., Bers, D.M., Banach, K., and Blatter, L.A. (2010). Isoform-and tissue-specific regulation of the Ca2+-sensitive transcription factor NFAT in cardiac myocytes and heart failure. American Journal of Physiology-Heart and Circulatory Physiology **298,** H2001-H2009. https://doi.org/10.1152/ajpheart.01072.2009
Sanna, B., Bueno, O.F., Dai, Y.-S., Wilkins, B.J., and Molkentin, J.D. (2005). Direct and indirect interactions between calcineurin-NFAT and MEK1-extracellular signal-regulated kinase 1/2 signaling pathways regulate cardiac gene expression and cellular growth. Molecular and Cellular Biology **25,** 865-878. https://doi.org/10.1128/MCB.25.3.865-878.2005
Saucerman, J.J., and Bers, D.M. (2008). Calmodulin mediates differential sensitivity of CaMKII and calcineurin to local Ca 2+ in cardiac myocytes. Biophysical journal **95,** 4597-4612. https://doi.org/10.1529/biophysj.108.128728
Shen, T., Cseresnyés, Z., Liu, Y., Randall, W.R., and Schneider, M.F. (2007). Regulation of the nuclear export of the transcription factor NFATc1 by protein kinases after slow fibre type electrical stimulation of adult mouse skeletal muscle fibres. The Journal of physiology **579,** 535-551. https://doi.org/10.1113/jphysiol.2006.120048
Shibasaki, F., Price, E.R., Milan, D., and McKeon, F. (1996). Role of kinases and the phosphatase calcineurin in the nuclear shuttling of transcription factor NF-AT4. Nature **382,** 370-373. https://doi.org/10.1038/382370a0
Shin, S.-Y., Choo, S.-M., Kim, D., Baek, S.J., Wolkenhauer, O., and Cho, K.-H. (2006). Switching feedback mechanisms realize the dual role of MCIP in the regulation of calcineurin activity. FEBS letters **580,** 5965-5973. https://doi.org/10.1016/j.febslet.2006.09.064
Shin, S.-Y., Yang, H.W., Kim, J.-R., Do Heo, W., and Cho, K.-H. (2011). A hidden incoherent switch regulates RCAN1 in the calcineurin–NFAT signaling network. J Cell Sci **124,** 82-90. https://doi.org/10.1242/jcs.076034
Stemmer, P.M., and Klee, C.B. (1994). Dual calcium ion regulation of calcineurin by calmodulin and calcineurin B. Biochemistry **33,** 6859-6866. https://doi.org/10.1021/bi00188a015
Wilkins, B.J., and Molkentin, J.D. (2004). Calcium–calcineurin signaling in the regulation of cardiac hypertrophy. Biochemical and biophysical research communications **322,** 1178-1191. https://doi.org/10.1016/j.bbrc.2004.07.121
Xiang, Y., and Kobilka, B.K. (2003). Myocyte adrenoceptor signaling pathways. Science **300,** 1530-1532. https://doi.org/10.1126/science.1079206
Yang, J.H., Polanowska-Grabowska, R.K., Smith, J.S., Shields, C.W., and Saucerman, J.J. (2014). PKA catalytic subunit compartmentation regulates contractile and hypertrophic responses to β-adrenergic signaling. Journal of molecular and cellular cardiology **66,** 83-93. https://doi.org/10.1016/j.yjmcc.2013.11.001
Zou, Y., Komuro, I., Yamazaki, T., Kudoh, S., Uozumi, H., Kadowaki, T., and Yazaki, Y. (1999). Both Gs and Gi proteins are critically involved in isoproterenol-induced cardiomyocyte hypertrophy. Journal of Biological Chemistry **274,** 9760-9770. https://doi.org/10.1074/jbc.274.14.9760
Zou, Y., Yao, A., Zhu, W., Kudoh, S., Hiroi, Y., Shimoyama, M., Uozumi, H., Kohmoto, O., Takahashi, T., and Shibasaki, F. (2001). Isoproterenol activates extracellular signal–regulated protein kinases in cardiomyocytes through calcineurin. Circulation **104,** 102-108. https://doi.org/10.1161/hc2601.090987